Agile maneuvering with intelligent articulated vehicles: a control perspective ⋆

Maciej Marcin Michałek *

* *Institute of Automation and Robotics*
Poznan University of Technology (PUT), Poznań, Poland
(e-mail: maciej.michalek@put.poznan.pl)

Abstract: Articulated vehicles are the popular means of freight and public transportation. Current trends and development forecasts indicate an increase of their use in the near future, mainly for economic and environmental reasons. Modular High Capacity Vehicles and articulated urban buses are the examples of modern transportation solutions that require agile maneuvering in cluttered spaces. Since maneuvering with articulated vehicles is a highly non-intuitive and burdening process for human-drivers, it seems reasonable to equip this kind of vehicles with systems which provide (semi-) autonomous maneuvering capabilities. In this paper, we consider a modular cascade-like control design methodology that is applicable to intelligent articulated vehicles enabling them to perform complex maneuvers either through a driver-assistance system or in an autonomous control mode. First, we discuss key properties of the so-called N-trailer kinematics, and the correspondence between practical motion problems defined for articulated vehicles and their formulation in the control engineering language. Next, the modular cascade-like control system structure is presented which allows solving various control tasks in a unified manner for multi-body vehicles of different kinematic structures and any number of segments. Solutions to selected control problems are illustrated by numerical and experimental results.

Keywords: articulated vehicles, tractor-trailers (N-trailers), intelligent vehicles, wheeled mobile robots, kinematics, nonlinear cascade control

1. INTRODUCTION

Articulated vehicles are the popular means of freight and public transportation. According to the trends observed today and development forecasts one shall expect increasing demand in using longer multi-articulated vehicles in the near future, motivated mainly by the economic and environmental reasons, see Leduc (2009), Odhams et al. (2009), HTAS EMS (2014). The modular High Capacity Vehicles, multi-articulated urban buses, multi-trailer road-trains and tractor-trailers agricultural vehicles are the examples of modern transportation solutions that require agile maneuvering, often in highly cluttered workspaces. Maneuvering with long multi-articulated vehicles in the presence of constraints imposed on a vehicle state is inherently a highly nonlinear process, being non-intuitive and burdening for human-drivers, especially when complex maneuvers have to be performed within the long-term tasks characteristic to the agriculture, mining, and public or freight transportation. As a consequence, people more and more often decline or feel discouraged to take the transportation duties in these difficult working conditions. It seems, thus, reasonable and highly justified to equip the articulated vehicles with intelligent systems which would assist the drivers in performing complex maneuvers or even replace some hand-made work with (semi-) autonomous maneuvering capabilities. Indeed, one observes today an increasing trend to automate the articulated vehicles on various automation levels (see Society of Automotive Engineers (2016)), including the case of an autonomous motion recently proposed for the farm vehicles, terminal tractors, and the truck-semitrailer freight vehicles, see Fig. 1.

On the other side, kinematic models of nonholonomic articulated structures are complex dynamical systems, rich in interesting properties which explain why and under which conditions maneuvering with these structures is so difficult. To make the control design problem tractable in a general case, the models of articulated vehicles should be compact and generic in order to structure and simplify their analysis and usage. Moreover, the resultant control system is expected to be modular (in the context of various motion tasks), relatively simple in practical implementation (limited computational resources), and scalable with respect to the number of vehicle segments. All the mentioned requirements make the control design issue a challenging problem.

The aim of this paper is to review and generalize selected recent developments and results, mainly of the author and his co-workers, in the context of a modular cascade-like control design methodology for the multi-articulated nonholonomic ground vehicles. In Section 2, we discuss the key properties of the so-called N-trailer kinematics, addressing next (in Section 3) the correspondence between practical motion problems defined for articulated vehicles, and their formulation in the language of control engineering. Section 4 is devoted to a description of a modular and scalable cascade-like control system which allows

⋆ This work was supported by the Institute of Automation and Robotics, PUT, under the statutory fund No. 09/93/DSPB/0911.

Fig. 1. Examples of automated articulated vehicles: the Volvo's autonomous truck concept Vera (left), the Case IH's autonomous tractor-trailer concept (middle), and the Terberg's AutoTUG terminal tractor (right); sources of photos: images.volvotrucks.com, www.caseih.com, angletsurfphoto.info/?s=Special+Vehicles+Terberg (all the pictures by permission)

solving various motion control tasks in a unified manner for articulated vehicles of different kinematic structures and an arbitrary number of segments. Section 5 illustrates selected experimental results obtained with a laboratory-scale articulated vehicle. Comments and open problems are provided in Section 6.

2. MODELLING OF ARTICULATED VEHICLES

We will restrict the subsequent considerations to vehicle structures with fixed (non-steerable) wheels; for modelling of the multi-steering N-trailers a reader is referred, e.g., to Tilbury et al. (1995) and Orosco-Guerrero et al. (2002).

2.1 Kinematic configuration, parameters, and relationships

Let us consider the N-trailer vehicle presented schematically in Fig. 2. The vehicles comprises $N+1$ unicycle-like

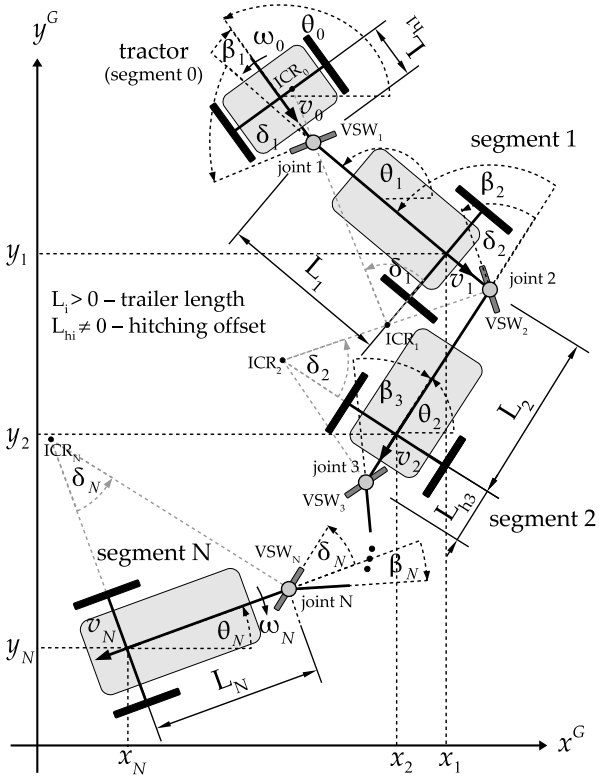

Fig. 2. Kinematic skeleton of an articulated N-trailer vehicle in a global frame $\{x^G, y^G\}$; θ_i is an orientation of segment ith

segments interconnected in an open kinematic chain by passive pivoting joints. The only active (driven) segment is a tractor numbered by 0, while any ith segment for $i = 1, \ldots, N$ is passive (non-driven). One distinguishes two types of kinematic parameters for this kind of vehicles: the segment length $L_i > 0$ and the hitching offset $L_{hi} \in \mathbb{R}$ for $i = 1, \ldots, N$. If $L_{hi} = 0$ than we say about the *on-axle hitching* for the ith connection; in the opposite case we say about the *off-axle hitching*. The off-axle hitching can be either with a positive offset ($L_{hi} > 0$) if the hitching point in located *behind* the wheels axle of a preceding segment, or with a negative offset ($L_{hi} < 0$) if the hitching point in located *in front of* the wheels axle of a preceding segment. Configuration of the N-trailer, uniquely describing a pose and a shape of the articulated vehicle, can be represented by the vector

$$\boldsymbol{q} = [\beta_1 \ \ldots \ \beta_N \ \theta_j \ x_j \ y_j]^\top \in \mathcal{Q} = \mathbb{T}^N \times \mathbb{R}^3, \qquad (1)$$

where $[\beta_1 \ \ldots \ \beta_N]^\top = \boldsymbol{\beta} \in \mathbb{T}^N$ consists of the joint angles

$$\beta_i \triangleq \theta_{i-1} - \theta_i, \qquad (2)$$

(see Fig. 2) and will be called the *shape configuration*, whereas $[\theta_j \ x_j \ y_j]^\top = \boldsymbol{q}_j \in \mathbb{R}^3$ will be called the *pose configuration* representing an orientation angle and position coordinates of a selected jth vehicle segment, $j \in \{0, \ldots, N\}$.

Motion of an every ith vehicle segment can be characterized by (pseudo-) velocity vector $\boldsymbol{u}_i = [\omega_i \ v_i]^\top \in \mathbb{R}^2$ comprising the angular velocity ω_i of a segment and a longitudinal velocity v_i of a mid-point of its wheels axle (see Fig. 2). For $i = 0$, one obtains the real kinematic control input in the form of tractor velocities $\boldsymbol{u}_0 = [\omega_0 \ v_0]^\top$.

Remark 1. Assumption about the unicycle-like vehicle segments is not very limiting. In the case where the tractor has got the rear-driven car-like kinematics the configuration vector (1) is usually extended with a steering-wheel angle $\beta_0 \in (-\pi/2; \pi/2)$, and the kinematic control input is redefined to $\boldsymbol{u} = [\zeta_0 \ v_0]^\top$, where ζ_0 is a steering rate of the front effective wheel. A correspondence between the unicycle control input $\boldsymbol{u}_0 = [\omega_0 \ v_0]^\top$ and the car-like control input $\boldsymbol{u}$ has been widely addressed – see, e.g., Michałek and Kozłowski (2012).

Upon elementary geometry, one can easily observe that the velocities of every two neighbouring segments are related by the following equation

$$\boldsymbol{u}_i = \underbrace{\begin{bmatrix} -\dfrac{L_{hi}}{L_i}\cos\beta_i & \dfrac{1}{L_i}\sin\beta_i \\ L_{hi}\sin\beta_i & \cos\beta_i \end{bmatrix}}_{\boldsymbol{J}_i(\beta_i)} \boldsymbol{u}_{i-1}, \qquad (3)$$

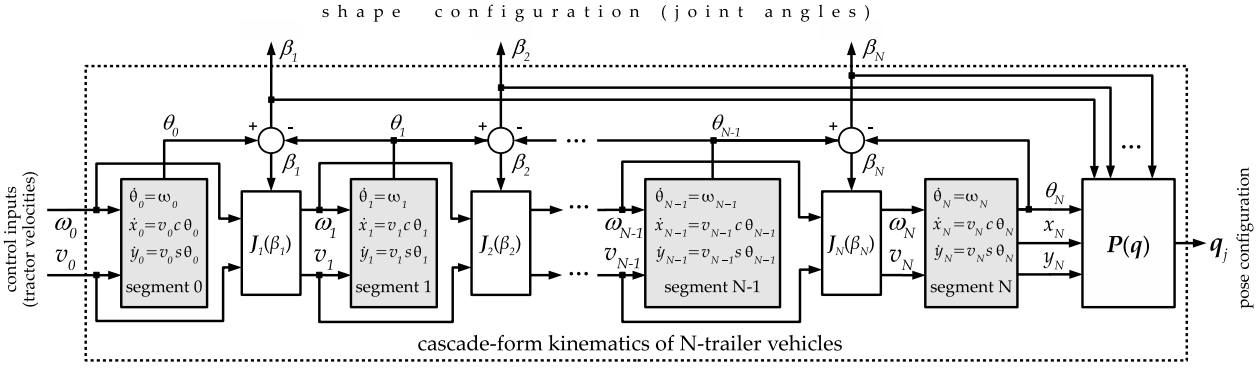

Fig. 3. Schematic representation of the cascade-form generic kinematic model of N-trailer vehicles with fixed wheels; the mapping $\boldsymbol{P}(\boldsymbol{q})$ allows transforming posture $\boldsymbol{q}_N$ to posture $\boldsymbol{q}_j$ of any selected jth vehicle segment, see Michałek and Pazderski (2018b)

where $\boldsymbol{J}_i(\beta_i)$ is a velocity transformation matrix having a well-determined inverse $\boldsymbol{J}_i^{-1}(\beta_i)$ if only $L_{hi} \neq 0$ allowing one to write

$$\boldsymbol{u}_{i-1} = \underbrace{\begin{bmatrix} -\dfrac{L_i}{L_{hi}}\cos\beta_i & \dfrac{1}{L_{hi}}\sin\beta_i \\ L_i\sin\beta_i & \cos\beta_i \end{bmatrix}}_{\boldsymbol{J}_i^{-1}(\beta_i)} \boldsymbol{u}_i. \tag{4}$$

Let us introduce the vectors $\boldsymbol{c}^\top = [1\ 0]$ and $\boldsymbol{d}^\top = [0\ 1]$, and an auxiliary matrix $\boldsymbol{\Gamma}_i(\beta_i) \triangleq \boldsymbol{I} - \boldsymbol{J}_i(\beta_i)$, where $\boldsymbol{I} \in \mathbb{R}^{2\times 2}$ is an identity matrix. Now, one can write $\omega_i = \boldsymbol{c}^\top \boldsymbol{u}_i$ and $v_i = \boldsymbol{d}^\top \boldsymbol{u}_i$. Thus, by time-differentiation of (2) we have

$$\begin{aligned} \dot\beta_i &= \omega_{i-1} - \omega_i = \boldsymbol{c}^\top [\boldsymbol{u}_{i-1} - \boldsymbol{u}_i] \\ &\overset{(3)}{=} \boldsymbol{c}^\top [\boldsymbol{J}_i^{-1}(\beta_i) - \boldsymbol{I}]\boldsymbol{u}_i = \boldsymbol{c}^\top \boldsymbol{\Gamma}_i(\beta_i)\boldsymbol{J}_i^{-1}(\beta_i)\boldsymbol{u}_i, \end{aligned} \tag{5}$$

which is valid for $i = 1, \ldots, N$. Kinematics of the jth vehicle segment, under the rolling-without-skidding motion conditions, can be described by the unicycle-like model

$$\dot{\boldsymbol{q}}_j \triangleq \begin{bmatrix} \dot\theta_j \\ \dot x_j \\ \dot y_j \end{bmatrix} = \begin{bmatrix} \boldsymbol{c}^\top \\ \boldsymbol{d}^\top\cos\theta_j \\ \boldsymbol{d}^\top\sin\theta_j \end{bmatrix} \begin{bmatrix} \omega_j \\ v_j \end{bmatrix} =: \boldsymbol{G}(\theta_j)\boldsymbol{u}_j. \tag{6}$$

Combination of (5) for $i = 1, \ldots, N$ and (6), together with transformation (3), leads to a generic kinematic model of the N-trailer in the form (see Michałek (2013b))

$$\begin{aligned} \dot\beta_1 &= \boldsymbol{c}^\top \boldsymbol{\Gamma}_1(\beta_1)\boldsymbol{u}_0, \\ \dot\beta_2 &= \boldsymbol{c}^\top \boldsymbol{\Gamma}_2(\beta_2)\boldsymbol{J}_1(\beta_1)\boldsymbol{u}_0, \\ &\vdots \\ \dot\beta_N &= \boldsymbol{c}^\top \boldsymbol{\Gamma}_N(\beta_N)\boldsymbol{J}_{N-1}(\beta_{N-1})\ldots\boldsymbol{J}_1(\beta_1)\boldsymbol{u}_0, \\ \dot{\boldsymbol{q}}_j &= \boldsymbol{G}(\theta_j)\boldsymbol{J}_j(\beta_j)\ldots\boldsymbol{J}_1(\beta_1)\boldsymbol{u}_0, \end{aligned}$$

where $\dot{\boldsymbol{q}}_0 = \boldsymbol{G}(\theta_0)\boldsymbol{u}_0$ for $j = 0$. The above set of equations can be rewritten in a more compact form as

$$\dot{\boldsymbol{q}} = \begin{bmatrix} \dot{\boldsymbol{\beta}} \\ \dot{\boldsymbol{q}}_j \end{bmatrix} = \begin{bmatrix} \boldsymbol{S}_\beta(\boldsymbol{\beta}) \\ \boldsymbol{S}_j(\boldsymbol{\beta}, \boldsymbol{q}_j) \end{bmatrix} \begin{bmatrix} \omega_0 \\ v_0 \end{bmatrix} = \boldsymbol{S}(\boldsymbol{q})\boldsymbol{u}_0 \tag{7}$$

$$= \boldsymbol{s}_1(\boldsymbol{q})\omega_0 + \boldsymbol{s}_2(\boldsymbol{q})v_0, \tag{8}$$

where $\boldsymbol{s}_1(\boldsymbol{q}), \boldsymbol{s}_2(\boldsymbol{q})$ are the columns of matrix $\boldsymbol{S}(\boldsymbol{q}) \in \mathbb{R}^{(N+3)\times 2}$, while $\boldsymbol{S}_\beta(\boldsymbol{\beta}) \in \mathbb{R}^{N\times 2}$ and $\boldsymbol{S}_j(\boldsymbol{\beta}, \boldsymbol{q}_j) \in \mathbb{R}^{3\times 2}$ are the shape- and pose-kinematics matrices, respectively, of the forms

$$\boldsymbol{S}_\beta(\boldsymbol{\beta}) = \begin{bmatrix} \boldsymbol{c}^\top\boldsymbol{\Gamma}_1(\beta_1) \\ \boldsymbol{c}^\top\boldsymbol{\Gamma}_2(\beta_2)\boldsymbol{J}_1(\beta_1) \\ \vdots \\ \boldsymbol{c}^\top\boldsymbol{\Gamma}_N(\beta_N)\boldsymbol{J}_{N-1}(\beta_{N-1})\ldots\boldsymbol{J}_1(\beta_1) \end{bmatrix}, \tag{9}$$

$$\boldsymbol{S}_j(\boldsymbol{\beta}, \boldsymbol{q}_j) = \boldsymbol{G}(\theta_j)\boldsymbol{J}_j(\beta_j)\ldots\boldsymbol{J}_1(\beta_1) \tag{10}$$

$$= \begin{bmatrix} \boldsymbol{c}^\top\boldsymbol{J}_j(\beta_j)\ldots\boldsymbol{J}_1(\beta_1) \\ \boldsymbol{d}^\top\boldsymbol{J}_j(\beta_j)\ldots\boldsymbol{J}_1(\beta_1)\cos\theta_j \\ \boldsymbol{d}^\top\boldsymbol{J}_j(\beta_j)\ldots\boldsymbol{J}_1(\beta_1)\sin\theta_j \end{bmatrix}. \tag{11}$$

The above modular formulation of the N-trailer kinematics can be graphically represented by the block scheme shown in Fig. 3. Compact nature of the model (7), together with particular properties of matrices $\boldsymbol{J}_i(\beta_i)$ and $\boldsymbol{G}(\theta_j)$, are very convenient, e.g., for the control design and stability analysis. According to the number M of the off-axle hitching present in a vehicle (corresponding to a number of $L_{hi} \neq 0$ in equation (9)), one distinguishes three main families of N-trailer vehicles (see Michałek (2012a)):

- the Standard N-Trailers (SNT) if $M = 0$,
- the Generalized N-Trailers (GNT) if $0 < M < N$,
- the non-Standard N-Trailers (nSNT) if $M = N$.

Properties of the N-trailer vehicles critically depend on the number M. This dependence will be discussed in the next subsection. It is worth to comment here that the SNT structures, mainly due to mechanical construction difficulties and lower maneuvering capabilities, are of much less practical importance (but of a theoretical significance) than the GNT and nSNT structures, which are widely applied in various transportation vehicles.

Following Altafini (2001), in every ith vehicle joint one can define the so-called *virtual steering wheel* illustrated in Fig. 4, which determines an instantaneous direction of longitudinal velocity μ_i of the ith joint. The ith virtual steering angle comes from the equation (cf. Altafini (2001))

$$\delta_i(\beta_i, \kappa_{i-1}) \triangleq \beta_i - \arctan\left(L_{hi}\kappa_{i-1}\right), \tag{12}$$

where

$$\kappa_{i-1} \triangleq \omega_{i-1}/v_{i-1} \tag{13}$$

is a motion curvature of a preceding $(i-1)$ segment. One can easily show that a motion curvature of the ith segment can be expressed with the virtual steering angle, that is,

$$\kappa_i = \frac{1}{L_i}\tan\delta_i \overset{(12)}{=} \frac{1}{L_i}\tan\left(\beta_i - \arctan\left(L_{hi}\kappa_{i-1}\right)\right), \tag{14}$$

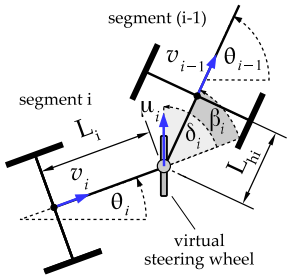

Fig. 4. Kinematic pair of two neighbouring segments and the concept of a virtual steering wheel, Altafini (2001)

which is valid for $i = 1, \ldots, N$; for $i = 0$ the motion curvature of the tractor reduces to $\kappa_0 = \omega_0/v_0$. Note that (14) is a recursive formula with respect to (w.r.t) a curvature, that is, $\kappa_i = \kappa_i(\beta_i, \kappa_{i-1})$ if $L_{hi} \neq 0$.

2.2 Kinematic properties of articulated vehicles

Articulated vehicles are very specific systems because their kinematics combine numerous interesting properties which are sources of their complex behaviour, and explain why maneuvering with N-trailers is so difficult and non-intuitive for human-drivers. The N-trailers belong to rare examples of systems which are both practically important and theoretically interesting, having a potential of joining both the industrial as well as academic communities. We will review the key properties of the N-trailers dividing them into those properties characterizing (7) as a dynamical system, and those more related to control design problems.

System-related properties: Kinematics (7) is a two-input nonlinear driftless dynamical system, with a dense set $\mathcal{E}$ of equilibria, that is, $\mathcal{E} = \{(\boldsymbol{q}, \boldsymbol{u}_0) : \ \boldsymbol{q} \in \mathcal{Q}, \boldsymbol{u}_0 = \boldsymbol{0}\}$. It is also nonholonomic in nature – kinematics (7) is valid only if all the vehicle wheels are purely rolling without skidding, that is, when the $N+1$ nonintegrable constraints $\dot{x}_i \sin\theta_i - \dot{y}_i \cos\theta_i = 0$ are satisfied for all $i = 0, 1, \ldots, N$. The number of configuration variables is (much) less than the number of control inputs, i.e., $\dim(\boldsymbol{q}) - \dim(\boldsymbol{u}_0) = N + 3 - 2 = N + 1$. The latter property makes some researchers call the N-trailers *underactuated systems*, Altafini (2001). Note, however, that the term *underactuation* is usually reserved in mechanics for those systems which have got more degrees of freedom (DOF) than control inputs; it does not hold in the case of kinematics (7) because DOF $= N + 3 - (N + 1) = 2 = \dim(\boldsymbol{u}_0)$ where $N + 1$ denotes the number of nonholonomic constraints. Note also, that the shape-kinematics, represented by subsystem $\dot{\boldsymbol{\beta}} = \boldsymbol{S}_\beta(\boldsymbol{\beta})\boldsymbol{u}_0$ has a lower-triangular structure which is useful, e.g., in the stability analysis.

In the case of nSNT kinematics, a multiple usage of velocity mapping (4) allows one to rewrite (7) with any other velocity vector $\boldsymbol{u}_i$, $i > 0$, treated as a control input. For example, if one is interested to express nSNT kinematics with $\boldsymbol{u}_N$ viewed as an input, the application of mapping (4) leads to

$$\boldsymbol{u}_0 = \prod_{i=1}^{N} \boldsymbol{J}_i^{-1}(\beta_i)\boldsymbol{u}_N,$$

and by substituting the right-hand side of the latter formula into (7) in place of $\boldsymbol{u}_0$ gives $\dot{\boldsymbol{q}} = \boldsymbol{S}(\boldsymbol{q}) \prod_{i=1}^{N} \boldsymbol{J}_i^{-1}(\beta_i)\boldsymbol{u}_N$ with an upper-triangular structure of the matrix $\boldsymbol{S}^*_\beta(\boldsymbol{\beta}) = \boldsymbol{S}_\beta(\boldsymbol{\beta}) \prod_{i=1}^{N} \boldsymbol{J}_i^{-1}(\beta_i)$ in the form

$$\boldsymbol{S}^*_\beta(\boldsymbol{\beta}) = \begin{bmatrix} \boldsymbol{c}^\top \boldsymbol{\Gamma}_1(\beta_1)\boldsymbol{J}_1^{-1}(\beta_1)\boldsymbol{J}_2^{-1}(\beta_2)\ldots\boldsymbol{J}_N^{-1}(\beta_N) \\ \boldsymbol{c}^\top \boldsymbol{\Gamma}_2(\beta_2)\boldsymbol{J}_2^{-1}(\beta_2)\ldots\boldsymbol{J}_N^{-1}(\beta_N) \\ \vdots \\ \boldsymbol{c}^\top \boldsymbol{\Gamma}_N(\beta_N)\boldsymbol{J}_N^{-1}(\beta_N) \end{bmatrix}.$$

Note that the above upper-triangular form cannot be so flexibly obtained for the SNT nor GNT kinematics, since for any $L_{hi} = 0$ the corresponding transformation matrix $\boldsymbol{J}_i(\beta_i)$ is singular. This unique property of the nSNT structure, which will be directly used to the control design purposes in Section 4, was a motivation of Michałek (2012a) to distinguish the nSNT kinematics from a wider set of the N-trailers classified in the literature before, see Altafini (2001); Lizarraga et al. (2001).

Some important properties of kinematics (7) critically depend on the signs of hitching offsets $L_{hi} \neq 0$ together with a sign of the tractor longitudinal velocity v_0 (that is, the sign of the second control input). These properties can be explained by addressing stability of a practically important equilibrium of shape-kinematics characterized by $\boldsymbol{\beta} = \boldsymbol{0}$ (zero-equilibrium), and corresponding to the steady motion conditions where the tractor moves with a constant non-zero input $\boldsymbol{u}_0 = [0 \ V]^\top$, $V = \text{const}$ and all the vehicle segments are lined-up. In other words, we consider under which conditions the vehicle chain will has a tendency to fold in (one or more) joints. This property was addressed by a simulation case study for the N-trailers already in Martinez et al. (2008), while it was formally investigated for a general case in Michałek (2013b). Computing a Taylor approximation of kinematics (7) around the steady motion conditions corresponding to $\boldsymbol{\beta} = \boldsymbol{0}, \theta_j = 0$ and $\boldsymbol{u}_0 = [0 \ V]^\top$, with a constant velocity $V \neq 0$, leads to the following, locally valid, transfer functions

$$G_{01}(s) \triangleq \frac{\beta_1(s)}{\omega_0(s)} = \frac{K_1}{(1 + \frac{L_1}{V}s)},$$

$$G_{0i}(s) \triangleq \frac{\beta_i(s)}{\omega_0(s)} = \frac{K_i}{(1 + \frac{L_i}{V}s)} \cdot \prod_{j=1}^{i-1} \frac{(1 - \frac{L_{hj}}{V}s)}{(1 + \frac{L_j}{V}s)}, \quad i \geq 2,$$

where $K_j = (L_j + L_{hj})/V$ is a static gain for the jth joint angle dynamics. One easily verifies that the joint angles will diverge from the point $\boldsymbol{\beta} = 0$ if the velocity $V < 0$ (structural instability in backward motion). This is a well known vehicle-folding effect observable during reversing with trailers. What is more interesting, the numerator of $G_{0i}(s)$ is a polynomial having a positive real zero if only $(L_{hj}/V) > 0$. In particular, for $V > 0$ (forward motion of a vehicle) and $L_{hi} > 0$, the positive zeros of transfer function $G_{0i}(s)$ for $i \geq 2$ make $G_{0i}(s)$ the non-minimum-phase (NMP) dynamics. Every off-axle hitching in a vehicle chain adds additional zero to $G_{0i}(s)$. As a consequence, in the response of joint angles $\beta_i(t)$ for $i \geq 2$ one shall expect such phenomena as (see Seron et al. (1997); Hoagg and Bernstein (2007)) an initial undershoot, initial oscillations (and zero crossings) or even an overshoot (despite the presence of strictly real poles in $G_{0i}(s)$), which can be dangerous for the vehicle and its neighbourhood when

maneuvering in tight cluttered workspaces. The exemplary responses of the joint angles for the nS3T kinematics have been presented in Fig. 5, where the grey lines denote responses of approximated linear dynamics G_{0i} for $i = 1, 2, 3$, whereas dark lines correspond to experimental data obtained with a laboratory-scale nS3T vehicle. One clearly

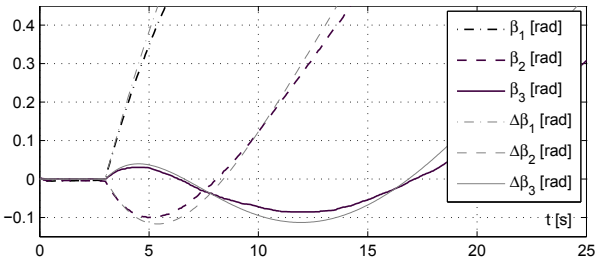

Fig. 5. Transients of the joint angles of nS3T kinematics in forward motion conditions: the response to an angular velocity ω_0 step-change applied at $t \approx 3\,\mathrm{s}$ (grey lines: simulations of approximated linear dynamics; dark lines: experimental data)

observes undershoot in the second joint angle, and initial oscillations (with two zero crossings) for the third joint angle. According to results presented in Michałek (2013b), the non-minimum-phase effects are amplified along a vehicle chain if $(L_{hi}/L_i) \geq 1$ and attenuated along a chain if $(L_{hi}/L_i) < 1$. Similar effects are observed for orientation angles $\theta_i(t)$ of the vehicle segments explainable upon a form of the transfer function

$$H_{0i}(s) \triangleq \frac{\theta_i(s)}{\omega_0(s)} = \frac{1}{s} \cdot \prod_{j=1}^{i} \frac{(1 - \frac{L_{hj}}{V} s)}{(1 + \frac{L_j}{V} s)}, \quad i \geq 1.$$

Control-related properties: A level of difficulty in controlling the N-trailer kinematics can be inferred in part by analysing a change in degrees of Lie brackets of the basic vector fields $\boldsymbol{s}_1(\boldsymbol{q})$ and $\boldsymbol{s}_2(\boldsymbol{q})$ introduced in (8) for various subsets of the configuration space $\mathcal{Q}$. In the works of Jean (1996) and Altafini (2001), it was shown that the highest degree of a Lie bracket needed to span the configuration space (the degree of nonholonomy) increases in the singular configurations $\boldsymbol{q}_s \in \mathcal{Q}_s \subset \mathcal{Q}$ determined by the zero-measure set

$$\mathcal{Q}_s = \left\{ \boldsymbol{q} : \left(\beta_i = \frac{\pi}{2} \mod \pi \right) \cup \left(\delta_l = \frac{\pi}{2} \mod \pi \right) \right\},$$

for any $i \in \{1, \ldots, N-1\}$ and any virtual steering angle δ_l defined by (12) with indexes l belonging to the index set I_{off} corresponding to the off-axle interconnections in the N-trailer vehicle (for the SNT kinematics $\delta_i \equiv \beta_i$, cf. (12), thus the second condition used in the definition of $\mathcal{Q}_s$ reduces to the first one). One shall expect that maneuvering with the N-trailers in the singular configurations becomes more difficult than in regular configurations. Local controllability of the N-trailer (7) in regular configurations, i.e. for $\boldsymbol{q} \in \mathcal{Q} \setminus \mathcal{Q}_s$, was proven by Altafini (2001) for the GNT kinematics, and in both regular and singular configurations by Laumond (1993) and Jean (1996) for the SNT kinematics (see also Barraquand and Latombe (1993) and a generalization to the n-bar system in Li and Respondek (2011)).

Structural instability of the shape-kinematics in backward motion conditions, and especially the NMP property of angular dynamics (discussed above) in forward motion due to the presence of the positive hitching offsets impose fundamental limitations on the achievable control performance with the N-trailers – a more detailed treatment can be found for nonlinear systems in Aguiar et al. (2008), for the N-trailers in Michałek (2013b), and also for linear systems in Hoagg and Bernstein (2007), Seron et al. (1997). Let us stress here that the NMP property makes the *forward* tracking with positive hitching offsets a challenging control problem for the nSNT and GNT kinematics if the guidance point is located on the trailer. Solutions to this problem have been recently provided, e.g., in Leng and Minor (2017) and Michałek and Pazderski (2018b).

Finally, let us consider the *differential flatness* property introduced and addressed in the context of N-trailers by Rouchon et al. (1993) and next extended by Li and Respondek (2012). The two-input system (8) is differentially flat if there exist two differentially independent functions f_1, f_2 (the *flat outputs*), generally dependent on $\boldsymbol{q}$, $\boldsymbol{u}_0$, and possibly time-derivatives of $\boldsymbol{u}_0$, such that all the configuration variables $\boldsymbol{q}$ and control inputs $\boldsymbol{u}_0$ can be expressed by the flat outputs f_1, f_2 and (possibly) their time-derivatives up to some order. According to the work of Rouchon et al. (1993), the SNT kinematics is differentially flat. The most popular flat outputs in this case are position coordinates (x_N, y_N) of the last trailer; other possible flat outputs for the SNT kinematics have been revealed in Li and Respondek (2012). It is well known that the differential flatness property reduces the problem of finding an admissible reference trajectory or reference path for the complex N-trailer system (8) to a simpler problem of finding a sufficiently smooth trajectory/path for the flat outputs only. From the control point of view, the differentially flat SNT kinematics can be transformed into a canonical model called the chained system, as it was shown in Sørdalen (1993), and is feedback linearizable by a dynamic feedback. Due to the mentioned benefits, differential flatness of the SNT vehicles was widely exploited in the problems of motion planning and feedback control design by various investigators. Unfortunately, the GNT and nSNT kinematics are generally not differentially flat. An exception is when a vehicle is a 1-trailer and comprises only a single off-axle hitching ($N = M = 1$), or in a multi-trailer vehicle where any two successive hitching in a vehicle chain are both not of the off-axle type, see Rouchon et al. (1993) and Morin and Samson (2008a), Minguez et al. (2008), Pradalier and Usher (2008). For the N-trailers with more than one successive off-axle hitching ($M > 1$) the differential flatness is lost, and the kinematics (8) is no more feedback-equivalent to a linear system. In this case, the reference signals computations (see, e.g., Michałek and Pazderski (2018a)), motion planning, and feedback control design for system (8) become the non-trivial problems. Until recently, the literature on these topics was relatively rare, and new results are still needed. Section 4 illustrates selected results in the context of feedback control for the non-flat nSNT vehicles.

Remark 2. Qualitative differences between the on-axle and off-axle interconnections in the N-trailers (and, to some extent, also consequences of a flatness loss) can be explained upon the form of iterative formula (14) relating curvatures of the neighbouring vehicle segments. Let us introduce the *inverse posture mapping* (using a short notation $\mathrm{c}\alpha \equiv \cos\alpha$, $\mathrm{s}\alpha \equiv \sin\alpha$)

$$\mathrm{inv}\boldsymbol{Q}(\boldsymbol{q}_i,\beta_i)=\begin{bmatrix}\theta_i+\beta_i\\ x_i+L_i\mathrm{c}\theta_i+L_{hi}\mathrm{c}(\theta_i+\beta_i)\\ y_i+L_i\mathrm{s}\theta_i+L_{hi}\mathrm{s}(\theta_i+\beta_i)\end{bmatrix}, \tag{15}$$

which comes from elementary geometrical arguments (see Fig. 2 and Michałek and Pazderski (2018b)), and allows one to compute a posture of the $(i-1)st$ segment $\boldsymbol{q}_{i-1}=\mathrm{inv}\boldsymbol{Q}(\boldsymbol{q}_i,\beta_i)$ upon a given posture of the ith segment $\boldsymbol{q}_i$ and a known joint angle β_i. In the context of flatness, let us discuss if it is possible to infer an instantaneous posture $\boldsymbol{q}_{i-1}$ and a motion curvature κ_{i-1} of a preceding vehicle segment and a shape (corresponding to angle β_i) of the segments pair upon a knowledge of only an instantaneous posture $\boldsymbol{q}_i$ and a motion curvature κ_i for the ith vehicle segment ($i>0$). An answer to this question depends on the interconnection type (on-axle/off-axle) between the segments. In the case of on-axle hitching (that is, for $L_{hi}=0$) the curvature of the ith vehicle segment depends solely on the joint angle β_i: if one knows κ_i then the angle β_i can be computed directly upon (14). Next, one can use mapping (15) to compute $\boldsymbol{q}_{i-1}$. By repeating this procedure it is possible to reconstruct any posture $\boldsymbol{q}_j$ and any angle β_j for $0\leq j<i$. On the other hand, for the on-axle hitching it is not possible to infer both components of velocity $\boldsymbol{u}_{i-1}$ directly upon velocity $\boldsymbol{u}_i$, even if the angle β_i is available [1]. This is a direct consequence of the fact that ω_{i-1} does not have any direct influence on components of velocity $\boldsymbol{u}_i$ leading to a singularity of matrix $\boldsymbol{J}_i(\beta_i)$, see (3) and (4). All the conclusions discussed above for the case of on-axle hitching can be summarized as follows:

$$\text{on-axle:}\quad \left\{\begin{matrix}\kappa_i\\ \boldsymbol{q}_i\end{matrix}\right\}\begin{matrix}\overset{(14)}{\Longrightarrow}\\ \Longleftrightarrow\end{matrix}\left\{\begin{matrix}\beta_i\\ \boldsymbol{q}_i\end{matrix}\right\}\overset{\mathrm{inv}\boldsymbol{Q}}{\Longrightarrow}\boldsymbol{q}_{i-1}\,, \tag{16}$$

$$\text{on-axle:}\quad \left\{\begin{matrix}\boldsymbol{u}_i\\ \beta_i\end{matrix}\right\}\overset{(4)}{\Longrightarrow}\boldsymbol{u}_{i-1}\,, \tag{17}$$

For the off-axle hitching case, the iterative formula (14) combines both the joint angle β_i and the motion curvature κ_{i-1} of a preceding segment. Hence, it is not possible to compute both β_i and κ_{i-1} using only (14). The latter obstruction is more fundamental because, indeed, the same motion curvature κ_i can be obtained for infinitely many combinations of a joint angle β_i and a motion curvature κ_{i-1}. As a consequence, it is not possible in this case to uniquely determine $\boldsymbol{q}_{i-1}$ upon the assumed piece of knowledge about the ith segment. On the other hand, in contrast to the on-axle hitching case, the transformation matrix $\boldsymbol{J}_i(\beta_i)$ is non-singular now, and one can infer velocity $\boldsymbol{u}_{i-1}$ directly upon velocity $\boldsymbol{u}_i$ by using (4) if the angle β_i is available. (If β_i is not available, it is not possible to infer neither $\boldsymbol{u}_{i-1}$ nor κ_{i-1} upon the assumed piece of knowledge about the ith segment.) The above considerations can be summarized as follows:

$$\text{off-axle:}\quad \left\{\begin{matrix}\kappa_i\\ \boldsymbol{q}_i\end{matrix}\right\}\begin{matrix}\overset{(14)}{\not\Longrightarrow}\\ \Longleftrightarrow\end{matrix}\left\{\begin{matrix}\beta_i\\ \boldsymbol{q}_i\end{matrix}\right\}\overset{\mathrm{inv}\boldsymbol{Q}}{\not\Longrightarrow}\boldsymbol{q}_{i-1}\,, \tag{18}$$

$$\text{off-axle:}\quad \left\{\begin{matrix}\boldsymbol{u}_i\\ \beta_i\end{matrix}\right\}\overset{(4)}{\Longrightarrow}\boldsymbol{u}_{i-1}\,. \tag{19}$$

By comparing (16)-(17) with (18)-(17), one can observe that the on-axle hitching is more beneficial in inferring postures of particular segments along a vehicle chain, while the off-axle hitching is more beneficial in inferring velocities of particular segments along a vehicle chain. The latter capability will be directly used to the purpose of cascade-like control system design addressed in Section 4.

[1] Although, $\boldsymbol{u}_{i-1}(t)$ can be inferred upon $\boldsymbol{u}_i(t)$ and $\beta_i(t)$ by using additionally the time derivative $\dot{\kappa}_i(t)$, if it is available.

3. MOTION TASKS AND CONTROL PROBLEMS

This section discusses five types of motion tasks being defined for the N-trailer vehicles followed by the more formally defined corresponding control problems.

3.1 A guidance point of a vehicle

A vehicle pose configuration represented by vector $\boldsymbol{q}_j=[\theta_j\ x_j\ y_j]^\top$ in (1) usually represents the vehicle segment which consists of variables measurable by a vehicle localization system. Selection of $\boldsymbol{q}_j$ is therefore not completely free, but it is rather determined by a particular localization system used for a vehicle. From the control problem point of view, one usually has to define the so-called *guidance point* for a vehicle, which represents a point of the most importance in the context of a motion task considered. Let us define the guidance point by some pose configuration $\boldsymbol{q}_l=[\theta_l\ x_l\ y_l]^\top$, which can be either fixed to the vehicle (being a pose of a vehicle segment for $l\in\{0,\ldots,N\}$) or located outside the vehicle body, see Lizarraga et al. (2001) , or can be even configuration-dependent as in Michałek (2015). Most of the motion tasks and control problems will be defined w.r.t. this point, which will be the main output of the system (7), that is (cf. Fig. 3),

$$\boldsymbol{y}\triangleq\boldsymbol{q}_l=\boldsymbol{H}(\boldsymbol{q})\in\mathbb{R}^3, \tag{20}$$

where the output mapping $\boldsymbol{H}(\boldsymbol{q})$ takes the form

$$\boldsymbol{H}=\begin{cases}[\boldsymbol{0}_{3\times N}\ \boldsymbol{I}_{3\times 3}]\,\boldsymbol{q} & \text{if } l=j\\ \mathrm{inv}\boldsymbol{Q}(\underbrace{\ldots\mathrm{inv}\boldsymbol{Q}(\boldsymbol{q}_j,\beta_j),\ldots}_{\boldsymbol{q}_{l+1}},\beta_{l+1}) & \text{if } l<j\\ \boldsymbol{Q}(\underbrace{\ldots\boldsymbol{Q}(\boldsymbol{q}_j,\beta_{j+1}),\ldots}_{\boldsymbol{q}_{l-1}},\beta_l) & \text{if } l>j\end{cases} \tag{21}$$

determined with the inverse posture mapping (15) and the *direct posture mapping* (see Michałek and Pazderski (2018b))

$$\boldsymbol{Q}(\boldsymbol{q}_{i-1},\beta_i)=\begin{bmatrix}\theta_{i-1}-\beta_i\\ x_{i-1}-L_i\mathrm{c}(\theta_{i-1}-\beta_i)-L_{hi}\mathrm{c}\theta_{i-1}\\ y_{i-1}-L_i\mathrm{s}(\theta_{i-1}-\beta_i)-L_{hi}\mathrm{s}\theta_{i-1}\end{bmatrix} \tag{22}$$

such that $\boldsymbol{q}_i=\boldsymbol{Q}(\boldsymbol{q}_{i-1},\beta_i)$. In general, $\boldsymbol{q}_l$ and $\boldsymbol{q}_j$ can concern poses of two different vehicle segments. Moreover, selection of the guidance point $\boldsymbol{q}_l$ may depend on a control problem under consideration and on a required vehicle motion strategy (forward/backward). The most commonly selected guidance points for the classical control tasks (like the stabilization at a point, trajectory-tracking, and path-following) are fixed to $l=N$ (the last trailer) or $l=0$ (the tractor unit).

In the case where only joint angles $\boldsymbol{\beta}$ are important from the control objective viewpoint, the output is defined as

$$\boldsymbol{y}\triangleq\boldsymbol{\beta}=[\boldsymbol{I}_{N\times N}\ \boldsymbol{0}_{N\times 3}]\,\boldsymbol{q}\in\mathbb{R}^3. \tag{23}$$

3.2 Docking with a trailer: the point-stabilization problem

The task of docking with the last trailer relies on placing the last vehicle segment in a constant target (reference)

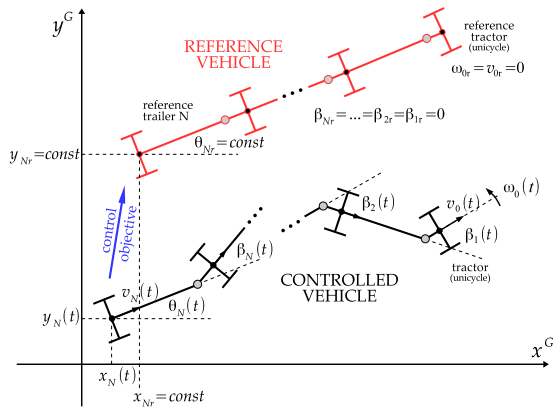

Fig. 6. Explanation of the point-stabilization problem for the case of $\boldsymbol{\beta}_r = \mathbf{0}$

pose $\boldsymbol{q}_{Nr} = [\theta_{Nr}\ x_{Nr}\ y_{Nr}]^\top$ and keep it in the steady state after reaching the target pose. This problem naturally arises, e.g., in the parking for loading/unloading tasks of freight articulated trucks or in positioning of a rear-mounted pantograph in electric articulated buses. Such a formulation of the docking task is an input-output control problem for the main output defined by (20) for $l = N$. One can complement this task by the requirement of moving the joint angles $\boldsymbol{\beta}$ to some predefined constant reference $\boldsymbol{\beta}_r$. In general, $\boldsymbol{\beta}_r$ can be arbitrary, but such a control problem is extremely difficult, especially for differentially non-flat N-trailer kinematics (see, e.g., Morin and Samson (2008b), Lizarraga et al. (2001), and Vendittelli and Oriolo (2000)). A simpler special case is when $\boldsymbol{\beta}_r = \mathbf{0}$ which corresponds to the lined all the vehicle segments up in the terminal configuration $\boldsymbol{q}_r = [\mathbf{0}^\top\ \boldsymbol{q}_{Nr}^\top]^\top$. This problem has been illustrated in Fig. 6. In order to formally define the point-stabilization (PS) problem let us introduce the stabilization error

$$\boldsymbol{e}_{\mathrm{ps}}(t) := \begin{bmatrix} \tilde{\boldsymbol{\beta}}(t) \\ \boldsymbol{e}_N(t) \end{bmatrix} \triangleq \begin{bmatrix} \boldsymbol{\beta}_r - \boldsymbol{\beta}(t) \\ \boldsymbol{q}_{Nr} - \boldsymbol{q}_N(t) \end{bmatrix} \in \mathcal{Q}, \qquad (24)$$

where $\tilde{\boldsymbol{\beta}}(t)$ is the shape-error, whereas $\boldsymbol{e}_N(t)$ is the pose-error.

Definition 3. (PS control problem). Given a bounded reference configuration $\boldsymbol{q}_r = [\boldsymbol{\beta}_r^\top\ \boldsymbol{q}_{Nr}^\top]^\top = \mathrm{const}$ (i.e., $\dot{\boldsymbol{q}}_r \equiv \mathbf{0}$), find a feedback control law $\boldsymbol{u}_0 = \boldsymbol{u}_0(\boldsymbol{q}_r, \boldsymbol{q}, \cdot)$ for the N-trailer kinematics (7), which makes a response of the closed-loop system $\dot{\boldsymbol{q}} = \boldsymbol{S}(\boldsymbol{q})\boldsymbol{u}_0(\boldsymbol{q}_r, \boldsymbol{q}, \cdot)$ bounded and convergent in the sense that: $\forall\, t \geq 0\ \ \|\boldsymbol{e}_{\mathrm{ps}}(t)\| < \infty$ and $\forall\, t \geq T\ \ \|\boldsymbol{e}_{\mathrm{ps}}(t)\| \leq \delta$ for some vicinity $\delta \geq 0$, some control time-horizon $T \in [0; \infty)$, and for all initial conditions $\boldsymbol{e}_{\mathrm{ps}}(0) \in \mathcal{E}_0 \subseteq \mathcal{Q}$.

In the above definition, the asymptotic convergence corresponds to $\delta = 0$, while the practical convergence to $\delta > 0$. Since the N-trailer kinematics is a nonholonomic driftless system, the PS control problem cannot be solved for $\delta = 0$ neither by using linear approximation methods nor by any continuous pure state feedback law, see Brockett et al. (1982) and Zabczyk (1989).

3.3 Moving in time: the trajectory-tracking problem

When the articulated vehicle has to track some (usually preprogrammed) time-varying configuration $\boldsymbol{q}_r(t) = [\boldsymbol{\beta}_r^\top(t)\ \boldsymbol{q}_{lr}^\top(t)]^\top$, called the reference trajectory, the motion task requires synchronization of motion geometry with a time flow leading to the trajectory-tracking problem. An example of such a task is tracking the moving harvester tip by one of the vehicle trailers during the agricultural field works. In this case, the harvester tip determines only an instantaneous reference pose $\boldsymbol{q}_{lr}(t)$ for the selected lth vehicle segment which must be currently filled with a grain. Therefore, tracking the pose $\boldsymbol{q}_{lr}(t)$ is the main input-output control objective here. The corresponding reference shape-configuration $\boldsymbol{\beta}_r(t)$ must be found upon the reference pose $\boldsymbol{q}_{lr}(t)$ in a way to satisfy constraints imposed by model (7). For the differentially non-flat kinematics (nSNT and GNT) such a compatible reference shape-configuration $\boldsymbol{\beta}_r(t)$ could be searched as a solution of the following exogenous system

$$\dot{\boldsymbol{\beta}}_r(t) = \boldsymbol{S}_\beta(\boldsymbol{\beta}_r(t)) \prod_{i=1}^{l} \boldsymbol{J}_i^{-1}(\beta_{ir}(t))\boldsymbol{u}_{lr}(t), \qquad (25)$$

where the matrix $\boldsymbol{S}_\beta$ has been determined by (9), while $\boldsymbol{u}_{lr}(t)$ is a given function of time corresponding to the reference pose $\boldsymbol{q}_{lr}(t)$ through unicycle kinematics similar to (6). Except the simplest cases of rectilinear and circular reference pose trajectories, finding a closed-form solution of (25) seems impossible. Moreover, finding $\boldsymbol{\beta}_r(t)$ is non-trivial also because it is a non-unique problem. For instance, if the reference pose $\boldsymbol{q}_{lr}(t)$ is time-periodic there exist probably at least 2^N number of different reference shape-trajectories $\boldsymbol{\beta}_r(t)$ corresponding to the same reference evolution of pose $\boldsymbol{q}_{lr}(t)$. This issue has been recently explained by Michałek and Pazderski (2018a), where eight different shape-configurations $\boldsymbol{\beta}_r$ were computed for the 3-trailer kinematics in the case of a circular motion of the last vehicle segment (every solution $\boldsymbol{\beta}_r$ corresponds to either folded or non-folded configuration of the ith joint, $i = 1, \ldots, N$). The question is how to find the only one expected reference shape-trajectory $\boldsymbol{\beta}_r(t)$ which does not involve any folding of an articulated vehicle (due to the presence of strict mechanical limitations in angular positions for joints in every practical articulated vehicle). In this context, the so called *segment-platooning* (S-P) reference trajectories $\boldsymbol{q}_r(t)$ have been introduced by Michałek (2017) and by Michałek and Pazderski (2018a), which additionally to equation (25) must satisfy the S-P condition

$$\forall\, \boldsymbol{\beta}_r(t) \quad v_{i-1r}(\boldsymbol{\beta}_r(t), \boldsymbol{u}_{lr}(t)) \cdot v_{ir}(\boldsymbol{\beta}_r(t), \boldsymbol{u}_{lr}(t)) > 0 \qquad (26)$$

for all $i = 1, \ldots, N$, where $v_{ir} = \boldsymbol{d}^\top \boldsymbol{u}_{ir}$ can be expressed with $\boldsymbol{u}_{lr}(t)$ and $\boldsymbol{\beta}_r(t)$ by using transformations (3) or (4), depending on whether $i > l$ or $i < l$. The S-P condition requires that all the reference segments of a reference vehicle must move with the same signs of their reference longitudinal velocities (i.e., all moving forward or all backward). Note that (26) prevents the folding effect for the reference N-trailer kinematics, and simultaneously leads to the persistently exciting reference trajectory with $\|\boldsymbol{u}_{lr}(t)\| > 0$ for all $t \geq 0$ and any $l \in \{0, \ldots, N\}$. Now, selection of an admissible shape-configuration $\boldsymbol{\beta}_r(t)$ for the nSNT kinematics is possible by checking the solutions of (25) for satisfaction of the S-P condition (26). The trajectory-tracking problem has been illustrated in Fig. 7. In order to formally define the trajectory-tracking (TT) problem let us introduce the tracking error

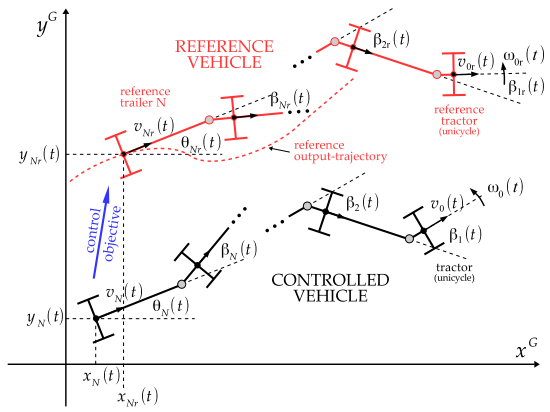

Fig. 7. Explanation of the trajectory-tracking problem with a guiding point located on the last trailer (i.e., for $l = N$)

$$\boldsymbol{e}_{\mathrm{tt}}(t) := \begin{bmatrix} \tilde{\boldsymbol{\beta}}(t) \\ \boldsymbol{e}_l(t) \end{bmatrix} \triangleq \begin{bmatrix} \boldsymbol{\beta}_r(t) - \boldsymbol{\beta}(t) \\ \boldsymbol{q}_{lr}(t) - \boldsymbol{q}_l(t) \end{bmatrix} \in \mathcal{Q}, \tag{27}$$

where $\tilde{\boldsymbol{\beta}}(t)$ is the shape-error, whereas $\boldsymbol{e}_l(t)$ is the pose-error.

Definition 4. (TT control problem). Given a preprogrammed (known a priori) bounded and sufficiently smooth reference trajectory $\boldsymbol{q}_r(t) = [\boldsymbol{\beta}_r^\top(t) \ \boldsymbol{q}_{lr}^\top(t)]^\top$ of the S-P type, find a feedback control law $\boldsymbol{u}_0 = \boldsymbol{u}_0(\boldsymbol{e}_{\mathrm{tt}}, t)$ for the N-trailer kinematics (7), which makes a response of the closed-loop error dynamics

$$\dot{\boldsymbol{e}}_{\mathrm{tt}} = \boldsymbol{S}(\boldsymbol{q}_r) \prod_{i=1}^{l} \boldsymbol{J}_i^{-1}(\beta_{ir}(t)) \boldsymbol{u}_{lr}(t) - \boldsymbol{S}(\boldsymbol{q}_r - \boldsymbol{e}_{\mathrm{tt}}) \boldsymbol{u}_0(\boldsymbol{e}_{\mathrm{tt}}, t)$$

bounded and convergent in the sense: $\forall\, t \geq 0 \ \ \| \boldsymbol{e}_{\mathrm{tt}}(t) \| < \infty$ and $\forall\, t \geq T \ \ \| \boldsymbol{e}_{\mathrm{tt}}(t) \| \leq \delta$ for some vicinity $\delta \geq 0$, some control time-horizon $T \in [0; \infty)$, and for all initial conditions $\boldsymbol{e}_{\mathrm{tt}}(0) \in \mathcal{E}_0 \subseteq \mathcal{Q}$.

In the above definition, the asymptotic tracking corresponds to $\delta = 0$, while the practical tracking corresponds to $\delta > 0$.

3.4 Moving along a path: the path-following problem

The task of following a predefined path is important for numerous practical applications. Simple examples include guiding a trailer along a road lane or guiding a trailer equipped with some implement along a passage on a field in agriculture. In contrast to the trajectory-tracking task, the time constraints are not directly imposed for the path-following task. In this case, time-parametrization of reference signals is either replaced by other kind of parametrization (usually by using a curvilinear path length) or the path is not parametrized at all, while instead it is represented in a form of a zero-level set of some two-dimensional function. Let us consider the latter case, which is a relatively new approach, used for the purpose of mobile robotics, e.g., in Morro et al. (2011), Consolini et al. (2010), and for the N-trailers in Michałek (2014b). In this approach the reference positional path is represented by a set of reference points

$$P_r \triangleq \{(x_{lr}, y_{lr}) : \ F(x_{lr}, y_{lr}) \triangleq \sigma f(x_{lr}, y_{lr}) = 0\}, \tag{28}$$

where $f(x_{lr}, y_{lr}) = 0$ determines equation of the reference geometrical path, whereas a sign of $\sigma \in \mathbb{R} \setminus \{0\}$ determines

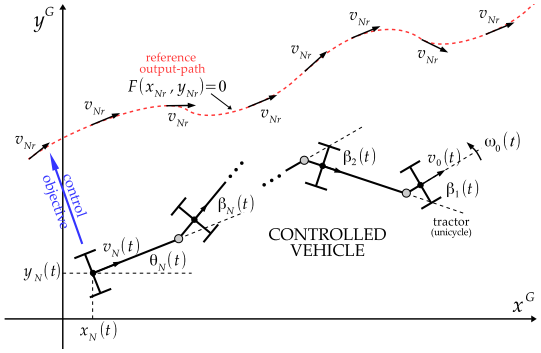

Fig. 8. Explanation of the path-following problem with a guiding point located on the last trailer (i.e., for $l = N$)

desired motion 'direction' along the reference path and its absolute value simultaneously scales the gradient of function F (one assumes that f is sufficiently smooth w.r.t its arguments). A reference orientation along the path is defined by a tangency angle

$$\theta_r(\boldsymbol{q}_{lr}) = \mathrm{Atan2c}\left(-\frac{\partial F(x_{lr}, y_{lr})}{\partial x_{lr}}, \frac{\partial F(x_{lr}, y_{lr})}{\partial y_{lr}} \right) \in \mathbb{R},$$

where $\mathrm{Atan2c}\,(\cdot,\cdot) : \mathbb{R} \times \mathbb{R} \to \mathbb{R}$ is a continuous counterpart of the four-quadrant $\mathrm{Atan2}\,(\cdot,\cdot) : \mathbb{R} \times \mathbb{R} \to (-\pi; \pi]$ function, see Michałek (2014b). Note that evaluating $F(\cdot,\cdot)$ at the current position (x_l, y_l) of a guidance point provides information about a signed (generally non-Euclidean) distance between the guidance point and the reference path; moreover, $F(x_l, y_l) = 0$ if and only if $(x_l, y_l) = (x_{lr}, y_{lr})$, that is only on the reference path. In contrast to the classical curvilinearly parametrized approach, one avoids in this way a necessity of finding the shortest distance to the path which may be problematic in practical applications. Definition of reference signals is complemented by imposing some (usually constant) reference longitudinal velocity $v_{lr} \neq 0$ for the guidance segment along the path. The path-following problem has been illustrated in Fig. 8. In order to formally define the path-following (PF) problem let us introduce the path-following error

$$\boldsymbol{e}_{\mathrm{pf}}(\boldsymbol{q}_l(t)) := \begin{bmatrix} \tilde{\boldsymbol{\beta}}(\boldsymbol{q}_l(t)) \\ \bar{\boldsymbol{e}}(\boldsymbol{q}_l(t)) \end{bmatrix} \triangleq \begin{bmatrix} \boldsymbol{\beta}_r(\boldsymbol{q}_l(t)) - \boldsymbol{\beta}(t) \\ \begin{bmatrix} \rho(\theta_r(\boldsymbol{q}_l(t)) - \theta_l(t)) \\ F(x_l(t), y_l(t)) \end{bmatrix} \end{bmatrix}, \tag{29}$$

where $\boldsymbol{e}_{\mathrm{pf}} \in \mathcal{Q}_{\mathrm{pf}} = \mathbb{T}^N \times (-\pi; \pi] \times \mathbb{R}$, $\rho : \mathbb{R} \to (-\pi; \pi]$ limits the orientation error to the bounded range, the terms $\theta_r(\cdot)$ and $F(\cdot,\cdot)$ have been determined at a current position of the guidance point of a vehicle, and the reference joint angles $\boldsymbol{\beta}_r$ have been related to the current pose $\boldsymbol{q}_l$ of the guidance segment (due to the lack of a parametrization). Generally, the reference angles $\boldsymbol{\beta}_r$ should be computed to conform to the S-P reference path (by analogy to the S-P trajectories addressed in Section 3.3). Finding a correspondence between $\boldsymbol{\beta}_r$ and $\boldsymbol{q}_l$ introduced in (29) is, however, very difficult (if possible at all). Fortunately, knowledge about the dependence $\boldsymbol{\beta}_r(\boldsymbol{q}_l(t))$ will not be necessary to application of the cascade-like control law discussed in Section 4.

Definition 5. (PF control problem). Given a preprogrammed (a priori known) S-P reference positional path determined by the zero-level set (28) and the reference velocity $v_{lr} \neq 0$, find a feedback control law $\boldsymbol{u}_0 = \boldsymbol{u}_0(\boldsymbol{e}_{\mathrm{pf}}, v_{lr})$ for the N-trailer kinematics (7), which makes the path-

following error (29) bounded and convergent in the sense that: $\forall\, t \geq 0 \;\; \| \boldsymbol{e}_{\rm pf}(\boldsymbol{q}_l(t))\| < \infty$ and $\forall\, t \geq T \;\; \| \boldsymbol{e}_{\rm pf}(\boldsymbol{q}_l(t))\| \leq \delta$ for some vicinity $\delta \geq 0$, some control time-horizon $T \in [0;\infty)$, and for all initial conditions $\boldsymbol{e}_{\rm pf}(\boldsymbol{q}_l(0)) \in \mathcal{E}_0 \subseteq \mathcal{Q}_{\rm pf}$.

The asymptotic path-following corresponds to $\delta = 0$, while the practical path-following corresponds to $\delta > 0$.

3.5 Keeping a lane: the averaged path-following problem

In the classical PF task discussed above, the reference positional path has to be followed only by a single selected vehicle segment, namely, by the guidance segment. In many practical applications, however, the reference path determines only a centre line for a motion corridor along which the *whole* multi-body articulated vehicle is expected to follow (at least in an averaged sense, see Altafini (2002, 2003) and Michałek (2015)); this corridor may be determined, e.g., by a width of a highway lane. Thus in this case, the motion problem is to follow within a corridor around the reference path, simultaneously minimizing a corridor-width occupied by the whole vehicle. This motion scenario has been graphically illustrated in Fig. 9, where $v_r \neq 0$ denotes a longitudinal velocity of a reference motion along the path. Minimization of the corridor-width

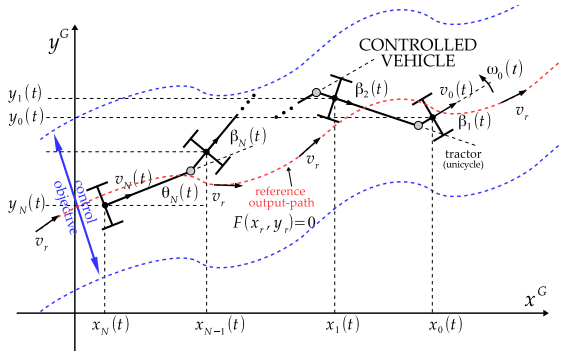

Fig. 9. Explanation of the averaged path-following problem; the red line denotes a positional reference path (represented as a level curve $F(x_r, y_r) = 0$), whereas the blue lines delimit a corridor around the path within which the whole articulated vehicle should stay during its motion

corresponds to minimization of the maximal off-track drawn by any of the vehicle segments. In order to formally define the averaged path-following (APF) problem let us consider a positional reference path, represented by a set

$$P_r \triangleq \{(x_r, y_r) : \; F(x_r, y_r) \triangleq \sigma f(x_r, y_r) = 0\}, \qquad (30)$$

$\sigma \in \mathbb{R}\setminus\{0\}$, and a corridor $B_\varepsilon \triangleq \bigcup_{(x_r,y_r)\in P_r} B(x_r, y_r, \varepsilon) \subset \mathbb{R}^2$ around the path, being a union of 2-dimensional balls $B(x_r, y_r, \varepsilon)$ centered at $(x_r, y_r) \in P_r$ and of some radius $\varepsilon > 0$ (see Fig. 10). Introduce also the off-track error $\boldsymbol{e}_i^{\perp}(x_r, y_r)$ for the ith vehicle segment, which is orthogonal to the path, see Fig. 10. A norm of $\boldsymbol{e}_i^{\perp}(x_r, y_r)$ corresponds to the shortest distance between position (x_i, y_i) of the ith vehicle segment and the path at point (x_r, y_r).

Definition 6. (APF control problem). Find a feedback control law $\boldsymbol{u}_0 = \boldsymbol{u}_0(\boldsymbol{q}, v_r)$ for the N-trailer kinematics (7), which guarantees that there exists a finite $T \geq 0$ such that $\forall\, t \geq T \;\; (x_i(t), y_i(t)) \in B_\varepsilon$ for all $i = 0, \ldots, N$, with a minimal possible resultant corridor radius

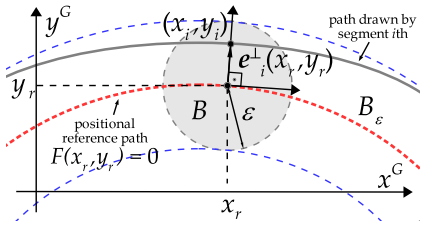

Fig. 10. Corridor B_ε around a reference path $F(x_r, y_r) = 0$ as a union of balls B of radius $\varepsilon > 0$ centered at $(x_r, y_r) \in P_r$

$$\varepsilon = \min\left(\max_{i=0,\ldots,N} \left\{ \sup_{(x_r,y_r)\in P_r} \left\| \boldsymbol{e}_i^{\perp}(x_r, y_r) \right\| \right\} \right). \qquad (31)$$

The APF control problem does not require (but does not exclude) asymptotic path-following by any of the vehicle segments, since it concerns the whole multi-body kinematic chain of a vehicle. There exist only two special cases of the APF which leads to $\varepsilon = 0$ (reducing the APF to the PF task), that is, for the rectilinear reference paths, and for the circular reference paths if additionally the vehicle has nSNT kinematics with $L_{hi} = L_i$ for all $i = 1, \ldots, N$, see Bushnell et al. (1994).

3.6 Aligning vehicle segments: the lining-up problem

The last motion task concerns aligning all the vehicle segments. Let us call it the lining-up (LU) problem, see Michałek (2014a). This is usually an auxiliary maneuver which shall help preparing a vehicle to subsequent complex motion tasks. In this case, the main output of kinematics (7) is a joint-angle vector $\boldsymbol{\beta}(t)$ as defined by (23), while evolution of a pose of any vehicle segment and a longitudinal velocity $v_r \neq 0$ of a maneuver should be bounded but besides that are of a secondary importance. The LU problem has been explained in Fig. 11. In order to formally

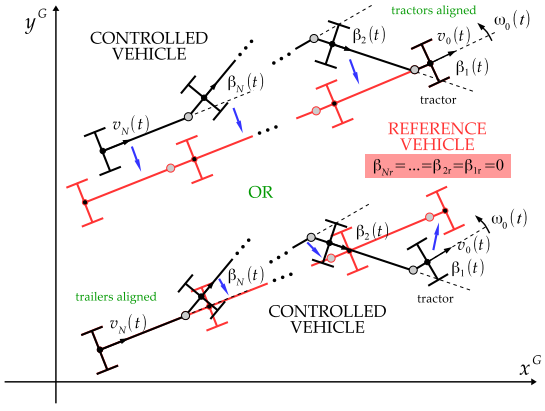

Fig. 11. Explanation of the lining-up problem for two possible initial conditions: where the tractor is initially aligned with a virtual reference tractor, and where the last trailer is aligned with a virtual reference trailer (virtual reference vehicles are highlighted in red)

define the LU problem let us introduce the lining-up error

$$\boldsymbol{e}_{\rm lu}(t) \triangleq [\boldsymbol{\beta}_r - \boldsymbol{\beta}(t)] \in \mathbb{T}^N \quad \text{with} \quad \boldsymbol{\beta}_r = \boldsymbol{0}. \qquad (32)$$

Definition 7. (LU control problem). Find a feedback control law $\boldsymbol{u}_0 = \boldsymbol{u}_0(\boldsymbol{e}_{\rm lu}, v_r) \equiv \boldsymbol{u}_0(\boldsymbol{\beta}, v_r)$ for the N-trailer kinematics (7), which makes the lining-up error (32) bounded

and convergent in the sense that: $\forall\, t \geq 0 \;\; \| \boldsymbol{e}_{\mathrm{lu}}(t)\| < \infty$ and $\forall\, t \geq T \;\; \| \boldsymbol{e}_{\mathrm{lu}}(t)\| \leq \delta$ for some vicinity $\delta \geq 0$, some control time-horizon $T \in [0; \infty)$, and for all initial conditions $\boldsymbol{e}_{\mathrm{lu}}(0) \in \mathcal{E}_0 \subseteq \mathbb{T}^N$.

The asymptotic lining-up corresponds to $\delta = 0$, while the practical lining-up to $\delta > 0$.

4. MODULAR CASCADE-LIKE CONTROL SCHEME

All the control problems defined in Section 3 can be solved with a modular cascade-like control system which will be introduced and discussed in the following subsections. A similar cascade-like control approach was used, e.g., in Chung et al. (2011) and Morales et al. (2013); it was applied there, however, under particular and limited motion conditions. If not stated otherwise, we will assume hereafter that $l = j = N$, thus the guidance point is located on the last trailer, the pose of which is measurable by a vehicle localization system.

4.1 A general control concept

The modular cascade-like control system for the N-trailer vehicles is presented in Fig. 12. One can distinguish two

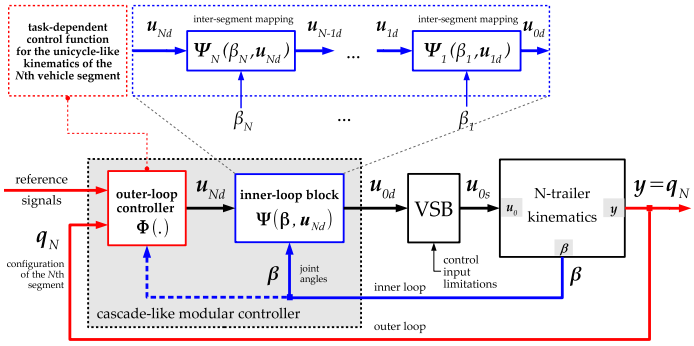

Fig. 12. Block scheme of the cascade-like modular control system for intelligent articulated vehicles (VSB: Velocity Scaling Block)

control loops in the system: the outer loop (highlighted in red) with a feedback from pose $\boldsymbol{q}_N$ of the last vehicle segment (treated here as a guiding segment), and the inner loop (highlighted in blue) with a feedback from the joint angles $\boldsymbol{\beta}$ (shape configuration). By this kind of a control system structure one divides the control problem, originally stated for the whole vehicle configuration, into a primary objective of guiding the Nth vehicle segment towards its reference pose, and a secondary objective of guaranteeing boundedness and terminal convergence of joint angles $\boldsymbol{\beta}$ to their corresponding reference values. In this approach the inner loop plays an auxiliary role for the primary control objective. From the theoretical viewpoint, the above strategy corresponds to the input-output control problem (with output $\boldsymbol{y} = \boldsymbol{q}_N$), where evolution of joint-angles can be viewed as a response of internal dynamics of the closed-loop system, see Isidori (1995) and Bolzern et al. (2001).

The main idea in the proposed control scheme from Fig. 12 relies on treating the guiding segment as a vehicle of unicycle-like kinematics (6) with virtual control input $\boldsymbol{u}_N$, and applying in the outer loop an appropriate (i.e., task-dependent) control function $\boldsymbol{\Phi}(\cdot)$ originally devised for the unicycle vehicle (numerous control functions of this type have been proposed in the literature for various control problems). The control function $\boldsymbol{\Phi}(\cdot)$ determines an instantaneous *desired* [2] velocity for the guidance segment, that is,

$$\boldsymbol{u}_{Nd} \triangleq \boldsymbol{\Phi}(\cdot). \tag{33}$$

Since the desired velocity (33) cannot be directly forced on the virtual input $\boldsymbol{u}_N$, the inner loop is responsible for transforming desired velocity (33) to the corresponding desired velocity $\boldsymbol{u}_{0d}$ for the tractor (active) unit by using some inter-segment mapping $\boldsymbol{\Psi}$, that is,

$$\boldsymbol{u}_{0d} \triangleq \boldsymbol{\Psi}(\boldsymbol{\beta}, \boldsymbol{u}_{Nd}) \overset{(33)}{=} \boldsymbol{\Psi}(\boldsymbol{\beta}, \boldsymbol{\Phi}(\cdot)). \tag{34}$$

In this manner, the tractor by executing desired velocities ω_{0d}, v_{0d} on its input $\boldsymbol{u}_0$ should force the guidance segment move like a unicycle vehicle controlled by the outer-loop control function $\boldsymbol{\Phi}(\cdot)$. The inter-segment mapping used in (34) can be defined as the following composition

$$\begin{aligned}\boldsymbol{\Psi} &\triangleq \boldsymbol{\Psi}_1(\beta_1, \boldsymbol{\Psi}_2(\beta_2, \ldots, \boldsymbol{\Psi}_{N-1}(\beta_{N-1}, \boldsymbol{\Psi}_N(\beta_N, \boldsymbol{u}_{Nd})) \ldots)) \\ &= (\boldsymbol{\Psi}_1 \circ \boldsymbol{\Psi}_2 \circ \ldots \circ \boldsymbol{\Psi}_N)(\boldsymbol{\beta}, \boldsymbol{u}_{Nd}),\end{aligned} \tag{35}$$

comprising the elementary inter-segment mappings

$$\boldsymbol{\Psi}_i(\beta_i, \boldsymbol{u}_{id}) = \begin{cases} \boldsymbol{\Psi}_i^{\mathrm{OFF}}(\beta_i, \boldsymbol{u}_{id}) & \text{if } L_{hi} \neq 0 \\ \boldsymbol{\Psi}_i^{\mathrm{ON}}(\beta_i, \boldsymbol{u}_{id}) & \text{if } L_{hi} = 0 \end{cases}, \tag{36}$$

for $i = 1, \ldots, N$, which map desired velocities between any two neighbouring segments, that is, $\boldsymbol{u}_{i-1d} = \boldsymbol{\Psi}_i(\beta_i, \boldsymbol{u}_{id})$. Particular forms of elementary inter-segment mappings introduced in (36) depend on the interconnection type. For the off-axle hitching in the ith joint one utilizes (4) and defines

$$\boldsymbol{\Psi}_i^{\mathrm{OFF}} \triangleq \boldsymbol{J}_i^{-1}(\beta_i)\boldsymbol{u}_{id} = \begin{bmatrix} -\dfrac{L_i}{L_{hi}}\mathrm{c}\beta_i\omega_{id} + \dfrac{1}{L_{hi}}\mathrm{s}\beta_i v_{id} \\ L_i\mathrm{s}\beta_i\omega_{id} + \mathrm{c}\beta_i v_{id} \end{bmatrix}, \tag{37}$$

whereas for the on-axle hitching in the ith joint one proposes to take

$$\boldsymbol{\Psi}_i^{\mathrm{ON}} \triangleq \begin{bmatrix} k_i(\beta_{id} - \beta_i) + \dot{\beta}_{id} + \omega_{id} \\ \xi\,|L_i\mathrm{s}\beta_i\omega_{id} + \mathrm{c}\beta_i v_{id}| \end{bmatrix} \tag{38}$$

with two design parameters $k_i > 0$ and $\xi \in \{-1, +1\}$, and with the *desired* (in contrast to the *reference*) joint angle

$$\beta_{id} \triangleq \mathrm{Atan2c}\,(L_i\omega_{id}\,\xi, v_{id}\,\xi) \in \mathbb{R}.$$

Note that (37) is a nonlinear but truly algebraic mapping, well-determined if only $L_{hi} \neq 0$. On the other hand, the first row of (38) defines an inner-loop control function, with a proportional part $k_i(\beta_{id} - \beta_i)$ the the feedforward part $\dot{\beta}_{id} + \omega_{id}$. A value of parameter ξ should be selected according to the expected vehicle motion strategy, that is, $\xi = +1$ for the forward motion, and $\xi = -1$ for the backward one.

Remark 8. A separate mapping $\boldsymbol{\Psi}_i^{\mathrm{ON}}$ has been introduced because in the case of on-axle hitching the transformation matrix $\boldsymbol{J}_i$ is singular and (37) is not well determined. However, in less demanding applications one can use, instead of (38), an alternative definition

$$\hat{\boldsymbol{\Psi}}_i^{\mathrm{ON}} \triangleq \hat{\boldsymbol{J}}_i^{-1}(\beta_i)\boldsymbol{u}_{id} = \begin{bmatrix} -\dfrac{L_i}{\epsilon_i}\mathrm{c}\beta_i\omega_{id} + \dfrac{1}{\epsilon_i}\mathrm{s}\beta_i v_{id} \\ L_i\mathrm{s}\beta_i\omega_{id} + \mathrm{c}\beta_i v_{id} \end{bmatrix} \tag{39}$$

[2] Note that, in general, $\boldsymbol{u}_{Nd}(t) \not\equiv \boldsymbol{u}_{Nr}(t)$, i.e., the *desired* velocity is not equivalent to the *reference* one (but the former can terminally converge to the latter).

being an approximation of (37) for some (sufficiently small) parameter $\epsilon_i \neq 0$. In practice, a 'size' of $|\epsilon_i|$ should be selected carefully by taking into account possible excessive amplification of feedback noises by using too small values for $|\epsilon_i|$.

It is worth emphasizing two key properties of the control system from Fig. 12:

- **Modularity** – the same unified structure of the cascade-like control system can be applied to various control tasks (addressed in Section 3), only by selecting an appropriate outer-loop control function $\boldsymbol{\Phi}(\cdot)$ specialized for the task under consideration and devised for unicycle-like kinematics of the guidance segment.
- **Scalability** – the same unified structure of the cascade-like control system can be applied to the N-trailer vehicles with an arbitrary number of segments; after changing the number of trailers, one needs only to change a number of inter-segment mappings (36) used in the inner-loop block (this operation can be easily automated if the information about the actual number of trailers is available).

The two properties mentioned above make the cascade-like system a fairly universal control framework for the N-trailers, which can be flexibly and relatively easily used in various practical applications.

4.2 Addressing control input limitations

Modularity of the control system can be complemented by the velocity scaling block (VSB), shown in Fig. 12, which allows preserving kinematic control-input limitations of a real vehicle. In the case of a unicycle-like tractor with the independent control inputs limited by

$$\forall\, t \geq 0 \;\; |\omega_0(t)| \leq \Omega \;\wedge\; |v_0(t)| \leq V, \tag{40}$$

for some finite upper bounds $\Omega > 0$, $V > 0$, one can apply a simple on-line scaling procedure

$$\boldsymbol{u}_{0s}(t) \triangleq \boldsymbol{u}_{0d}(t) / \max\left\{1, \frac{|\omega_{0d}(t)|}{\Omega}, \frac{|v_{0d}(t)|}{V}, \right\}, \tag{41}$$

which transforms the nominally computed desired velocities $\boldsymbol{u}_{0d}$ into the scaled ones $\boldsymbol{u}_{0s}$ already respecting limitations (40). Moreover, procedure (41) simultaneously preserve an instantaneous motion curvature of the tractor in the sense that $(\omega_{0s}/v_{0s}) = (\omega_{0d}/v_{0d})$. The scaling procedure (41) can be easily adopted to the case of a differentially-driven tractor (with a maximal wheel velocity $\omega_{\max}$ used as a limitation) and a car-like tractor, as it was explained, respectively, in Michałek and Kozłowski (2010) and Michałek and Kozłowski (2012).

4.3 Laboratory setup used for experimental verification

The next section illustrates selected results obtained using the laboratory setup designed and build in the Institute of Automation and Robotics at Poznan University of Technology. The set-up consists of the RMP robotic vehicle presented in Fig. 13, and an external vision-based localization system. The vehicle comprises a differentially-driven tractor and three off-axle hitched passive trailers (values of hitching offsets L_{hi} are adjustable in a range $[-0.008; 0.056]$ m allowing the vehicle to be reconfigured to the nS3T, G3T, or S3T kinematics). The tractor is equipped with a floating-point digital signal processor (TMS320F28335) and is computationally self-sufficient (all the control algorithms and a reference signals generator have been implemented on-board). The last trailer has been selected as a guiding segment which is localized by the vision system upon a view of a LED marker mounted on the trailer top. The angles β_i are measured with the 14-bit absolute encoders mounted in the joints. The on-board motion control system with a cascade-like controller (presented in Fig. 13) works with a frequency of 100 Hz. More details on the laboratory set-up can be found in Michałek et al. (2015).

5. CASCADE-LIKE CONTROL: THE RESULTS FOR NON-STANDARD-N-TRAILER KINEMATICS

We are going to illustrate application of the cascade-like control concept discussed in Section 4 to solve selected control problems for the N-trailer vehicles. Due to space limitations, we will limit our considerations only to the nSNT kinematics with $l = j = N$.

5.1 Application to the PS/TT/PF control problems

Application of the cascade-like control concept to three classical control problems (i.e. PS, TT, and PF) can be illustrated by a unified block scheme in Fig. 14. Specialization of the control system to a particular control task comes from a selection of an appropriate outer-loop control function $\boldsymbol{\Phi}(\cdot)$. Since $\boldsymbol{\Phi}(\cdot)$ determines desired velocities $\boldsymbol{u}_{Nd}$ for unicycle kinematics, one can find numerous functions of this type widely proposed in the literature for various control problems (see, e.g., Kim and Tsiotras (2002); Morin and Samson (2008a)). To fix our attention, let us limit further considerations to the VFO (Vector-Field-Orientation) control function which can be applied

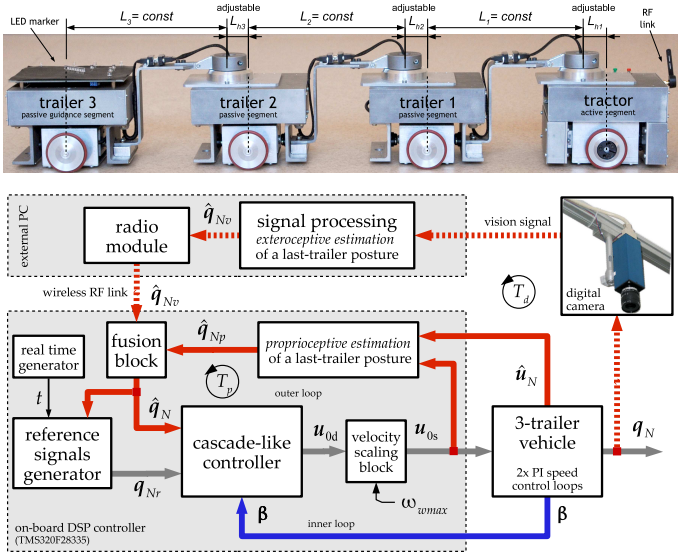

Fig. 13. The RMP robotic vehicle (upper view) available as a part of the laboratory setup in the Institute of Automation and Robotics at Poznan University of Technology, and a block schema of the control system (with an external vision feedback) implemented on the vehicle's board

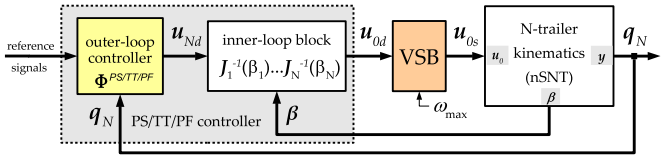

Fig. 14. Cascade-like control system for nSNT vehicles capable of solving the PS, TT, and PF control problems

in the outer loop for all three classical tasks in the versions proposed in Michałek and Kozłowski (2010) and Michałek and Gawron (2018).

In the VFO control approach, one assumes the existence of the so-called *convergence vector field* $\boldsymbol{h} = [h_\theta \; h_x \; h_y]^\top \in \mathbb{R}^3$, which at every point of the configuration space determines desired direction toward a reference pose. A form of the first component h_θ will be defined in the same manner for all the tasks, whereas the other two components $\bar{\boldsymbol{h}} = [h_x \; h_y]^\top \in \mathbb{R}^2$ will be defined separately for three considered control problems. Upon the VFO control design strategy, the VFO control function can be represented in the uniform manner as follows

$$\boldsymbol{\Phi}(\boldsymbol{h}) \triangleq \begin{bmatrix} h_\theta \\ h_x \mathrm{c}\theta_N + h_y \mathrm{s}\theta_N \end{bmatrix} \triangleq \begin{bmatrix} k_a(\theta_a - \theta_N) + \dot{\theta}_a \\ h_x \mathrm{c}\theta_N + h_y \mathrm{s}\theta_N \end{bmatrix}, \quad (42)$$

where $k_a > 0$ is a design parameter,

$$\theta_a \triangleq \mathrm{Atan2c}\,(\zeta\, h_y, \zeta\, h_x) \in \mathbb{R}$$

is an auxiliary orientation variable, and $\zeta \in \{-1, +1\}$ is a bi-valued decision factor determined separately for all three control tasks. Specialized VFO control functions are determined by specialized forms of vector fields $\bar{\boldsymbol{h}}$, that is, $\boldsymbol{\Phi}^{\mathrm{PS}} \triangleq \boldsymbol{\Phi}(\boldsymbol{h}^{\mathrm{PS}})$, $\boldsymbol{\Phi}^{\mathrm{TT}} \triangleq \boldsymbol{\Phi}(\boldsymbol{h}^{\mathrm{TT}})$, and $\boldsymbol{\Phi}^{\mathrm{PF}} \triangleq \boldsymbol{\Phi}(\boldsymbol{h}^{\mathrm{PF}})$ with

$$\bar{\boldsymbol{h}}^{\mathrm{PS}}(\bar{\boldsymbol{e}}_N) \triangleq k_p \bar{\boldsymbol{e}}_N - \zeta\eta \,\|\, \bar{\boldsymbol{e}}_N \|\, [\mathrm{c}\theta_{Nr} \; \mathrm{s}\theta_{Nr}]^\top, \quad (43)$$

$$\bar{\boldsymbol{h}}^{\mathrm{TT}}(\bar{\boldsymbol{e}}_N, t) \triangleq k_p \bar{\boldsymbol{e}}_N + [\dot{x}_{Nr} \; \dot{y}_{Nr}]^\top, \quad (44)$$

$$\bar{\boldsymbol{h}}^{\mathrm{PF}}(x_N, y_N) \triangleq k_p F(x_N, y_N)\boldsymbol{\vartheta} + v_r \boldsymbol{R}\boldsymbol{\vartheta}, \quad (45)$$

where

$$\bar{\boldsymbol{e}}_N \triangleq \begin{bmatrix} x_{Nr} - x_N \\ y_{Nr} - y_N \end{bmatrix}$$

is a positional error, $k_p > 0$ and $\eta \in (0, k_p)$ are the design parameters, $v_r > 0$ is an absolute value of the reference velocity $v_{Nr} = \zeta v_r$, $\boldsymbol{\vartheta} = -\nabla F / \|\nabla F\|$ is a negative gradient versor of function F, while $\boldsymbol{R} = \left[\begin{smallmatrix} 0 & 1 \\ -1 & 0 \end{smallmatrix}\right]$ is a fixed rotation matrix. The resultant cascade-like control law for the nSNT kinematics takes now the form

$$\boldsymbol{u}_{0d} \triangleq \prod_{i=1}^{N} \boldsymbol{J}_i^{-1}(\beta_i)\boldsymbol{\Phi}(\boldsymbol{h}), \quad \boldsymbol{h} \in \{\boldsymbol{h}^{\mathrm{PS}}, \boldsymbol{h}^{\mathrm{TT}}, \boldsymbol{h}^{\mathrm{PF}}\}, \quad (46)$$

where selection of the argument $\boldsymbol{h}$ depends on the particular control task under consideration.

Solution to the PS problem (stated in Definition 3) with control law (46) and the VFO control function $\boldsymbol{\Phi}^{\mathrm{PS}} = \boldsymbol{\Phi}(\boldsymbol{h}^{\mathrm{PS}})$ has been proposed in Michałek (2012a). The exemplary experimental results in backward docking obtained with the nS3T vehicle are provided in Fig. 15. One can observe non-oscillatory and fairly natural motion of a vehicle despite the fact that no motion planning between the initial and final configuration was done in this case. This is a result of the VFO control function properties (with the so-called *directing effect*) which smoothly (non-oscillatory) guides the last trailer to a reference pose. The non-folding motion of a vehicle chain is guaranteed here for the positive hitching offsets present in a vehicle; for the negative offsets, similar control performance shall be expected in forward docking maneuvers, see Michałek (2012a). The latter work shows also that the PS control problem can be solved for the nSNT kinematics with the VFO controller only with the practical convergence, that is for $\delta > 0$, although a value of vicinity δ can be made arbitrarily small.

Solution to the TT control task (see Definition 4) with control law (46) and the VFO control function $\boldsymbol{\Phi}^{\mathrm{TT}} = \boldsymbol{\Phi}(\boldsymbol{h}^{\mathrm{TT}})$ has been proposed in Michałek (2017), were sufficient conditions for asymptotic tracking were provided. Exemplary experimental results of backward tracking the eight-shaped (Lissajous curve) reference trajectory with the nS3T vehicle are presented in Fig. 16. A very difficult initial condition has been intentionally imposed on the vehicle in order to reveal control system ability to perform agile maneuvering in the closed-loop system during a transient stage. It is worth stressing that computation of the reference joint angles was not needed in this case, since the angles $\boldsymbol{\beta}_r(t)$ are not used in the cascade-like control system. This fact substantially simplifies application of the control law in practice. The non-folding motion of a vehicle chain is obtained, again, for the positive hitching offsets present in a vehicle; for the negative offsets, similar

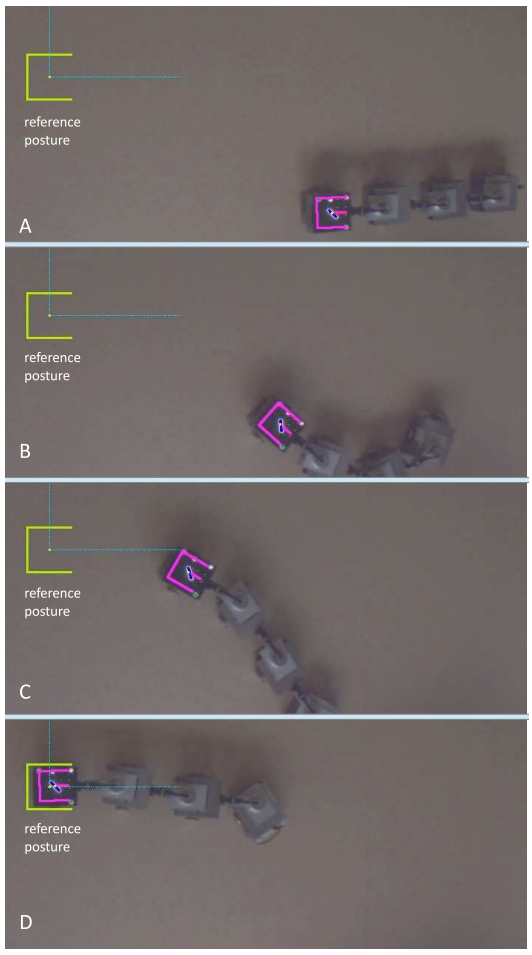

Fig. 15. A sequence of upper-camera views of experimental docking maneuvers obtained with the RMP laboratory vehicle (a reference pose has been denoted by the green dock, a detected pose of the last trailer has been denoted by the purple mark)

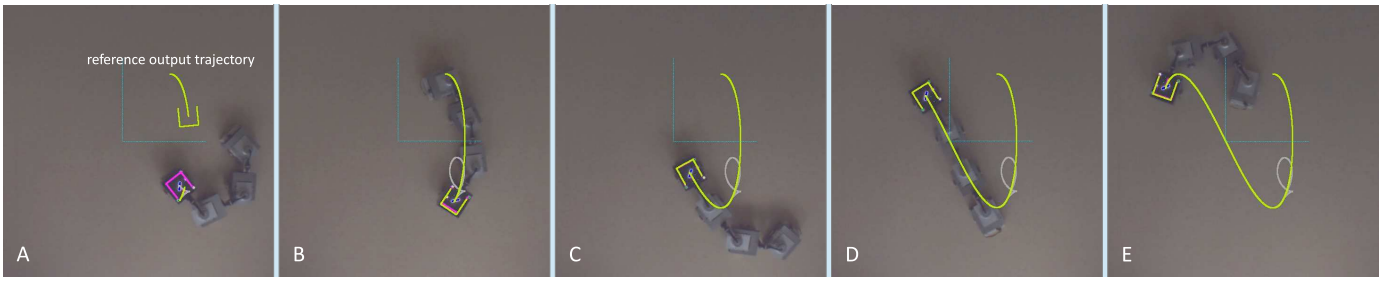

Fig. 16. A sequence of upper-camera views of experimental tracking the eight-shaped reference trajectory (highlighted in green) with the RMP laboratory vehicle (a detected pose of the last trailer has been denoted by the purple mark); a trajectory drawn by the last trailer has been denoted in grey

control performance shall be expected in forward tracking maneuvers, see Michałek (2017).

Solution to the PF control problem (formulated by Definition 5) for the nSNT kinematics, with sufficient conditions for asymptotic stability of point $\boldsymbol{e}_{\rm pf} = \boldsymbol{0}$ in the closed-loop system, has been studied in Michałek (2014b). The results provided there illustrate control quality with an alternative outer-loop control function $\boldsymbol{\Phi}(\cdot)$ proposed by Morro et al. (2011). Figure 17 presents (for the first time) selected experimental results obtained with the VFO control function $\boldsymbol{\Phi}^{\rm PF} = \boldsymbol{\Phi}(\boldsymbol{h}^{\rm PF})$ determined by the vector field (45). We concern the case of backward following an elliptical reference path (represented by the zero-level set $f(x_{Nr}, y_{Nr}) \triangleq (x_{Nr}^2/a^2)+(y_{Nr}^2/b^2)-1 = 0$) with an initial vehicle configuration located relatively far from the reference path. Similarly to the TT problem, no computation of the reference joint angles $\boldsymbol{\beta}_r$ was needed in application of the cascade-like control system. Again, the non-folding motion of a vehicle chain is ensured for the positive hitching offsets, while for the negative offsets similar control performance shall be expected in forward maneuvers, see Michałek (2014b) for a formal justification.

5.2 Application to the APF control problem

In order to take into consideration the whole articulated vehicle in the task of averaged path-following, one needs to define a guiding point for the vehicle by combining information about all its segments in some sense. Following the concept proposed in Michałek (2015) for the forward motion conditions, let us introduce the so-called *virtual guidance point* (VGP) $\bar{\boldsymbol{q}} \in \mathbb{R}^3$, being a weighted combination of poses of all the vehicle segments, that is,

$$\bar{\boldsymbol{q}} = \left[\bar{\theta}_r \;\; \bar{x}_r \;\; \bar{y}_r\right]^\top \triangleq w_0\boldsymbol{q}_0 + \ldots + w_N\boldsymbol{q}_N,$$

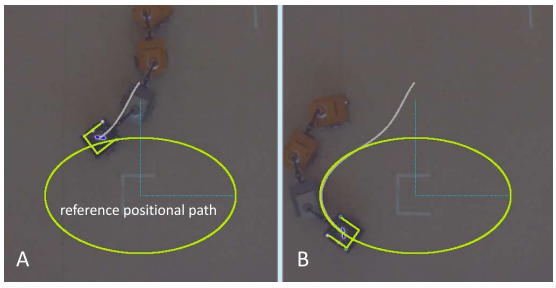

Fig. 17. A sequence of two selected upper-camera views illustrating experimental following of an elliptical reference path (the green line) with the RMP laboratory vehicle (the grey line denotes the path drawn by a last trailer of the vehicle)

where the weights

$$\boldsymbol{w} = [w_0 \; w_1 \; \ldots \; w_N]^\top \in \mathbb{R}^{N+1}_{\geq 0} : \; w_0 + \ldots + w_N = 1 \quad (47)$$

are treated as design parameters. Values of the weights shall be appropriately selected in order to minimize the off-track of a vehicle (see (31)) with respect to a given reference path represented by $F(\bar{x}_r, \bar{y}_r) = 0$, cf. (30). Postulating the unicycle-like motion nature of the VGP, i.e., assuming that $\dot{\bar{\boldsymbol{q}}} = \boldsymbol{G}(\bar{\theta})\bar{\boldsymbol{u}}$ for some virtual input $\bar{\boldsymbol{u}} = [\bar{\omega} \; \bar{v}]^\top$ and matrix $\boldsymbol{G}$ resulting from (6), one can easily derive (see Michałek (2015)) the desired velocity vector for the N-trailer in the form

$$\boldsymbol{u}_{0d} \triangleq \boldsymbol{\Gamma}^\dagger(\boldsymbol{q}, \boldsymbol{w})\boldsymbol{G}(\bar{\theta})\boldsymbol{\Phi}^{\rm APF}, \quad (48)$$

where the outer-loop function $\boldsymbol{\Phi}^{\rm APF} \triangleq \boldsymbol{\Phi}(\boldsymbol{h}^{\rm PF}(\bar{x}, \bar{y}))$ is determined by the vector field $\bar{\boldsymbol{h}}^{\rm PF}(\bar{x}, \bar{y})$ resulting from definition (45) and evaluated at a current position of VGP, whereas $\boldsymbol{\Gamma}^\dagger = (\boldsymbol{\Gamma}^\top\boldsymbol{\Gamma})^{-1}\boldsymbol{\Gamma}^\top$ is a left pseudo-inverse of a 3×2 matrix

$$\boldsymbol{\Gamma}(\boldsymbol{q}, \boldsymbol{w}) = w_0\boldsymbol{G}(\theta_0) + \sum_{i=1}^{N} w_i\boldsymbol{G}(\theta_i)\prod_{j=i}^{1}\boldsymbol{J}_j(\beta_j).$$

The resultant control system for the APF problem has been shown in Fig. 18. One can observe that the APF

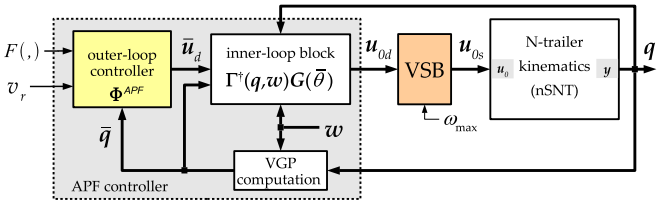

Fig. 18. Cascade-like control system for nSNT vehicles capable of solving the APF control problem in forward motion conditions (VGP: Virtual Guidance Point)

control problem is treated here in a similar way as the PF control problem, replacing only a guidance point fixed to a single segment with the virtual guidance point (VGP) combining poses of all the vehicle segments. The key issue is to select/find the weights $\boldsymbol{w}$ which lead to the minimal (or at least acceptably small) corridor radius ε introduced in Definition 6. Exemplary simulation results illustrating effectiveness of the proposed control strategy for the nS3T kinematics with negative hitching offsets ($L_{hi} = -0.1\,\mathrm{m}$, $i = 1, 2, 3$) have been presented in Fig. 19. The plots compare control performance for two cases: with $\boldsymbol{w} = [1 \; 0 \; 0 \; 0]^\top$ and with $\boldsymbol{w} = [0.3 \; 0.15 \; 0.55 \; 0.0]^\top$, where the latter weights were found off-line in the steady motion conditions of a vehicle obtained for a circular reference

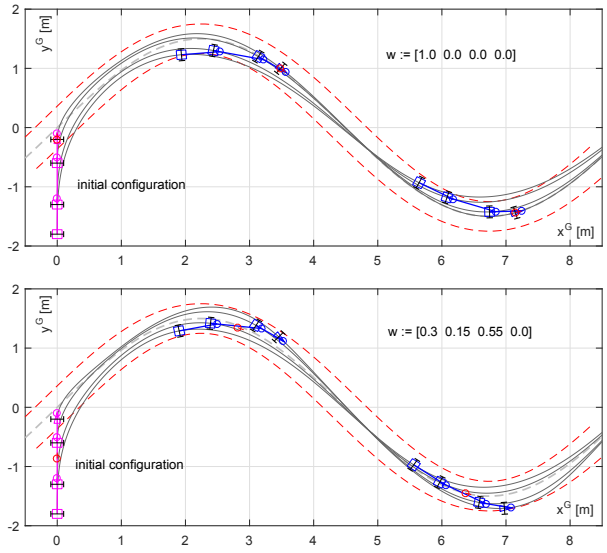

Fig. 19. Exemplary simulation results of the averaged path-following with nS3T in forward motion conditions along a sinusoidal path for two different weights vectors (the VGP has been highlighted by the red mark)

path of curvature $\kappa_r = 0.67\,\mathrm{m}^{-1}$. The red dashed lines in Fig. 19 delimit the ± 0.25 m-width corridor around the reference sinusoidal path. One can observe that selection of weights $\boldsymbol{w}^*$ allows the controller (48) to keep the paths drawn by all the vehicle segments within the imposed corridor (in contrast to the case where the tractor plays a role of a guidance segment, a shown on the upper plot in Fig. 19). It is worth stressing that in general the VGP is not fixed to the vehicle body, but it is floating since its pose depends on a current vehicle configuration. So far, the APF problem has been addressed for the N-trailers only in the case of forward motion conditions.

5.3 Application to the LU control problem

A commonly used practical method to solve this control problem relies on using the structural asymptotic stability of the point $\boldsymbol{\beta} = \mathbf{0}$ for the N-trailers in forward motion conditions. By forcing a zero-curvature forward motion to a tractor, the chain of vehicle segments will asymptotically (for $t \to \infty$) tend to line all the trailers up with the tractor unit – we will call this approach the *passive LU* control. In this approach, the tractor is a guiding segment. One can show, see Michałek (2014a), that a convergence rate of joint angles in the passive lining-up maneuver is (locally) inversely proportional to the trailer lengths and can be estimated upon the approximated dynamics $\dot{\boldsymbol{\beta}}(t) = \boldsymbol{W}_p\boldsymbol{\beta}(t)$ where $\mathrm{eig}(\boldsymbol{W}_p) = \{-V_0/L_i,\, i = 1,\ldots,N\}$ and $V_0 \in (0;\infty)$ is a prescribed longitudinal velocity of the tractor. Therefore, for a vehicle with long trailers the effective passive LU maneuver requires excessively long distance travelled by a tractor segment. An alternative approach is to apply the control system shown in Fig. 20 which allows lining all the nSNT vehicle segments up in an active manner – we will call this approach the *active LU* control. In this case, the last trailer is a guiding segment (the role replaced with a tractor), and the LU outer-loop feedback controller takes the form

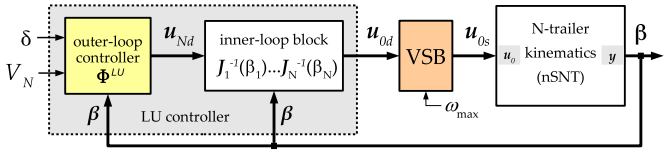

Fig. 20. Control system for nSNT vehicles capable of solving the *active LU* control problem

$$\boldsymbol{\Phi}^{\mathrm{LU}} \triangleq \begin{bmatrix} 0 \\ \Phi_v \end{bmatrix}, \quad \Phi_v \triangleq \begin{cases} -\mathrm{sgn}(L_{hN})\, V_N & \text{for } \|\boldsymbol{\beta}\| > \delta \\ 0 & \text{for } \|\boldsymbol{\beta}\| \le \delta \end{cases},$$

where $V_N \in (0;\infty)$ is a prescribed velocity of a maneuver for the last trailer. Function $\boldsymbol{\Phi}^{\mathrm{LU}}$ determines a zero-curvature motion for the last trailer in a backward strategy if $\mathrm{sgn}(L_{hN}) > 0$, and in a forward strategy if $\mathrm{sgn}(L_{hN}) < 0$. If an articulated vehicle is equipped with the sign-homogeneous hitching (that is, if $\mathrm{sgn}(L_{hN}) = \mathrm{sgn}(L_{hi})$ for all $i = 1,\ldots,N-1$) the LU control law

$$\boldsymbol{u}_{0d}(\boldsymbol{\beta}) \triangleq \prod_{i=1}^{N} \boldsymbol{J}_i^{-1}(\beta_i)\boldsymbol{\Phi}^{\mathrm{LU}} \tag{49}$$

solves the LU control problem from Definition 7 in the active manner for the nSNT kinematics in some (small) vicinity $\mathcal{E}_0$ of zero. It has been revealed in Michałek (2014a) that a convergence rate of joint angles during the active lining-up process can be estimated for sufficiently small joint angles upon the approximated dynamics $\dot{\boldsymbol{\beta}}(t) = \boldsymbol{W}_a\boldsymbol{\beta}(t)$ where $\mathrm{eig}(\boldsymbol{W}_a) = \{-V_N/|L_{hi}|,\, i = 1,\ldots,N\}$. Thus, for the vehicle with (much) shorter absolute hitching offsets than the trailer lengths (the most practical case) convergence of joint angles during the active lining-up maneuver can be (much) faster and more effective relative to a similar effect in the passive lining-up maneuver. As a consequence, a resultant distance travelled by the guiding segment can be (much) shorter in the active lining-up maneuver when compared with the passive one. Exemplary experimental results obtained for the active lining-up maneuver with the nS3T vehicle with hitching offsets $L_{hi} = -0.008\,\mathrm{m}$, $i = 1,2,3$, have been presented in Fig. 21. Since all the hitching offsets are negative in this case, the lining-up maneuver has been performed in forward motion conditions. It is worth noting a very short distance travelled by the last trailer during the maneuver, and (as a side effect of the lining-up strategy) a preservation of the orientation angle θ_N on its initial condition $\theta_N(0)$ during the whole control process. Additional results obtained also for the G3T and S3T kinematics can be found in Michałek (2014a).

6. COMMENTS AND OPEN PROBLEMS

We have introduced and discussed the modular and scalable nonlinear cascade-like control system which allows solving various motion control problems for the N-trailer kinematics in a unified way. The cascade-like structure simplifies a control design process, even for differentially non-flat nSNT and GNT kinematics, practically reducing it to the feedback control design for unicycle-like kinematics. In this way, one may avoid a difficult problem of computing the time-varying reference joint angles $\boldsymbol{\beta}_r$, which (as it has been shown and discussed above) are not needed for a practical execution of agile maneuvers with the N-trailers. Such a simplification must be followed,

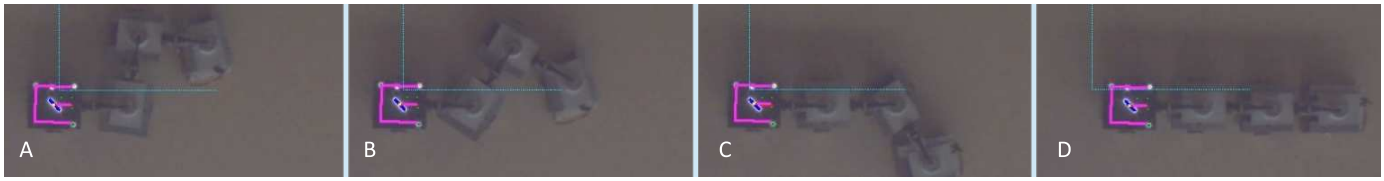

Fig. 21. A sequence of upper-camera views of the experimental active lining-up maneuver obtained with the RMP laboratory vehicle (a detected pose of the last trailer has been denoted by the purple mark)

however, by a guarantee that internal dynamics of joint angles is naturally stable to avoid the vehicle-folding effects, not detectable by the outer feedback loop (except the LU problem, no direct stabilization of joint-angle errors is applied in the proposed cascade-like control system). This guarantee imposes some fundamental constraints on a possible combinations of vehicle motion strategies (forward/backward) and signs of hitching offsets present in a vehicle chain. As a consequence of these constraints the PS, TT, and PF control problems are solved mainly for the backward motion conditions if all the hitching offsets are positive, or for forward motion strategy if all the hitching offsets are negative. Control design for the case of mixed signs of hitching offsets is challenging in general, especially when asymptotic convergence for the output error is addressed, see the recent paper by Michałek and Pazderski (2018b). Table 1 explains which control problems have been solved so far with the cascade-like control approach for particular kinematics of the N-trailers. Some of the publications include only simulation results, without providing any rigorous stability analysis for the closed-loop system (denoted by 'noA' in Table 1).

There still exist open issues in the area of control design for the N-trailers; selected problems can be formulated in a form of questions:

- How to stabilize the non-flat N-trailer kinematics at an *arbitrary* configuration $\boldsymbol{q}_r$?
- Is the nSNT/GNT kinematics controllable in singular configurations?
- How to compute the S-P reference configuration trajectories and paths for the non-flat GNT kinematics?
- Is the SNT kinematics inherently more sensitive to feedback noises relative to nSNT kinematics?
- How to solve the APF problem for backward motion conditions?
- How to address control problems for the N-trailers in the presence of state constraints preserving agile maneuvering capabilities?

In the case of state-constrained motion tasks formulated for the N-trailers (taking into account, e.g., obstacles in the motion environment, mechanical limits in the vehicle joints, and limited motion curvature of a tractor unit), it seems that the cascade-like feedback control system considered in this paper shall be treated only as a part of a larger motion-algorithmization system. This system should tightly combine constrained motion planning and feedback control in a one coherent system in order to preserve capability of performing agile maneuvers under difficult practical motion conditions. Probably only in this way the autonomous N-trailers will have a chance to be more widely accepted in practical applications.

ACKNOWLEDGEMENTS

The author thanks all his co-workers, in particular Marcin Kiełczewski and Tomasz Jedwabny for their contribution to the experimental part of the presented research. Selected results recalled in this paper were obtained under the following research grants: N N514 087038 (Polish Ministry of Science and Higher Education), 93/194/13 DS-MK (Faculty of Computing, PUT), and 2016/21/B/ST7/02259 (National Science Centre, Poland).

REFERENCES

Aguiar, A., Hespanha, J., and Kokotović, P. (2008). Performance limitations in reference-tracking and path-following for nonlinear systems. *Automatica*, 44(3), 598–610.

Altafini, C. (2001). Some properties of the general n-trailer. *Int. J. Control*, 74(4), 409–424.

Altafini, C. (2002). Following a path of varying curvature as an output regulation problem. *IEEE TAC*, 47(9), 1551–1556.

Altafini, C. (2003). Path following with reduced off-tracking for multibody wheeled vehicles. *IEEE TCST*, 11(4), 598–605.

Barraquand, J. and Latombe, J.C. (1993). Nonholonomic multibody mobile robots: controllability and motion planning in the presence of obstacles. *Algorithmica*, 10, 121–155.

Bolzern, P., DeSantis, R.M., and Locatelli, A. (2001). An input-output linearization approach to the control of an n-body articulated vehicle. *ASME Journal of DSMC*, 123, 309–316.

Brockett, R.W., Millman, R.S., and Sussmann, H.J. (1982). *Differential Geometric Control Theory*. Birkhäuser, Boston.

Bushnell, L., Mirtich, B., Sahai, A., and Secor, M. (1994). Off-tracking bounds for a car pulling trailers with kingpin hitching. In *33rd IEEE CDC*, 2944–2949. Lake Buena Vista, USA.

Chung, W., Park, M., Yoo, K., Roh, J.I., and Choi, J. (2011). Backward-motion control of a mobile robot with n passive off-hooked trailers. *J. Mech. Sci. Techn.*, 25(11), 2895–2905.

Consolini, L., Maggiore, M., Nielsen, C., and Tosques, M. (2010). Path following for the PVTOL aircraft. *Automatica*, 46, 1284–1296.

Hoagg, J.B. and Bernstein, D.S. (2007). Nonminimum-phase zeros. Much to do about nothing. *IEEE CSM*, 27(3), 45–57.

HTAS EMS (2014). Greening and safety assurance of future modular road vehicles. Book of requirements. Technical Report EUREKA, E! 6284-HTAS EMS, NL Innovatie.

Isidori, A. (1995). *Nonlinear Control Systems*. Springer, London.

Jean, F. (1996). The car with N trailers: characterisation of the singular configurations. *ESAIM: COCV*, 1, 241–266.

Kim, B.M. and Tsiotras, P. (2002). Controllers for unicycle-type wheeled robots: theoretical results and experimental validation. *IEEE TRA*, 18(3), 294–307.

Laumond, J.P. (1993). Controllability of a multibody mobile robot. *IEEE Trans. Robot. Autom.*, 9(6), 755–763.

Leduc, G. (2009). Longer and Heavier Vehicles. An overview of technical aspects. Technical Report EUR 23949 EN, European Commission, Joint Research Centre,Institute for Prospective Technological Studies, Luxembourg.

Leng, Z. and Minor, M.A. (2017). Curvature-based ground vehicle control of trailer path following considering sideslip and limited steering actuation. *IEEE TITS*, 18(2), 332–348.

Table 1. Published solutions/results for the N-trailers obtained with cascade-like controllers (the lack of a formal analysis has been denoted by 'noA')

↓task↓	SNT kinematics	GNT kinematics	nSNT kinematics
PS	Michałek and Kiełczewski (2014)	Michałek (2012a)-noA	Michałek (2012a), Michałek et al. (2015), Michałek and Kiełczewski (2015)
TT	Michałek (2012b)-noA	–	Yoo and Chung (2010), Chung et al. (2011), Michałek et al. (2015), Michałek (2017), Michałek and Kiełczewski (2017), Michałek and Pazderski (2018b)
PF	Michałek (2013a)-noA	Michałek (2013a)-noA	Michałek (2014b)
APF	–	–	Michałek (2015)-noA
LU	Michałek (2014a)-noA	Michałek (2014a)-noA	Michałek (2014a)

Li, S.J. and Respondek, W. (2011). The geometry, controllability, and flatness property of the n-bar system. *Int. J. Control*, 84, 834–850.

Li, S.J. and Respondek, W. (2012). Flat outputs of two-input driftless control systems. *ESAIM: COCV*, 18, 774–798.

Lizarraga, D., Morin, P., and Samson, C. (2001). Chained form approximation of a driftless system. Application to the exponential stabilization of the general N-trailer system. *Int. J. Control*, 74(16), 1612–1629.

Martinez, J.L., Morales, J., Mandow, A., and Garcia-Cerezo, A. (2008). Steering limitations for a vehicle pulling passive trailers. *IEEE Trans. Control Syst. Technol.*, 16(4), 809–818.

Michałek, M. (2012a). Application of the VFO method to set-point control for the N-trailer vehicle with off-axle hitching. *Int. J. Control*, 85(5), 502–521.

Michałek, M. (2012b). Tracking control strategy for the standard N-trailer mobile robot – a geometrically motivated approach. In K. Kozłowski (ed.), *Robot Motion and Control 2011*, volume 422 of *Lecture Notes in Control and Information Sciences*, 39–51. Springer.

Michałek, M. (2013a). Cascaded approach to the path-following problem for N-trailer robots. In *Proc. 9th Int. Workshop on Robot Motion and Control*, 161–166. Wasowo Palace, Poland.

Michałek, M. (2013b). Non-minimum-phase property of N-trailer kinematics resulting from off-axle interconnections. *Int. J. Control*, 86(4), 740–758.

Michałek, M. (2014a). Lining-up control strategies for N-trailer vehicles. *J Intell Robot Syst*, 75(1), 29–52.

Michałek, M. and Kiełczewski, M. (2014). Cascaded VFO set-point control for N-trailers with on-axle hitching. *IEEE Trans. Cont. Syst. Techn.*, 22, 1597–1606.

Michałek, M. and Kozłowski, K. (2010). Vector-Field-Orientation feedback control method for a differentially driven vehicle. *IEEE Trans. Cont. Syst. Techn.*, 18(1), 45–65.

Michałek, M. and Kozłowski, K. (2012). Feedback control framework for car-like robots using the unicycle controllers. *Robotica*, 30, 517–535.

Michałek, M.M. (2014b). A highly scalable path-following controller for N-trailers with off-axle hitching. *Control Eng. Practice*, 29, 61–73.

Michałek, M.M. and Kiełczewski, M. (2015). The concept of passive control-assistance for docking maneuvers with N-trailer vehicles. *IEEE/ASME Trans. Mechatronics*, 20, 2075–2084.

Michałek, M.M., Kiełczewski, M., and Jedwabny, T. (2015). Cascaded VFO control for non-standard N-trailer robots. *J Intell Robot Syst*, 77, 415–432.

Michałek, M.M. and Pazderski, D. (2018a). Computing the admissible reference state-trajectories for differentially non-flat kinematics of non-Standard N-Trailers. In *2018 European Control Conference (ECC)*, 551–556. Limassol,Cyprus.

Michałek, M.M. and Pazderski, D. (2018b). Forward tracking of complex trajectories with non-Standard N-Trailers of non-minimum-phase kinematics avoiding a jackknife effect. *Int. J. Control*, 1–14. DOI: 10.1080/00207179.2018.1448117.

Michałek, M. (2015). Motion control with minimization of a boundary off-track for non-Standard N-Trailers along forward-followed paths. In *2015 IEEE CASE*, 1564–1569. Gothenburg, Sweden.

Michałek, M. (2017). Cascade-like modular tracking controller for non-Standard N-Trailers. *IEEE TCST*, 25(2), 619–627.

Michałek, M. and Gawron, T. (2018). VFO path following control with guarantees of positionally constrained transients for unicycle-like robots with constrained control input. *J. Intell Robot Syst*, 89(1), 191–210.

Michałek, M. and Kiełczewski, M. (2017). Robustification of the modular tracking control system for non-Standard N-Trailers of uncertain kinematics. *Control Eng. Practice*, 64, 160–172.

Minguez, J., Lamiraux, F., and Laumond, J.P. (2008). Motion planning and obstacle avoidance. In B. Siciliano and O. Khatib (eds.), *Springer handbook of robotics*, 827–852. Springer.

Morales, J., Martinez, J.L., Mandow, A., and Gracia-Cerezo, A.J. (2013). Steering the last trailer as a virtual tractor for reversing vehicles with passive on- and off-axle hitches. *IEEE Trans. Industrial Electronics*, 60(12), 5729–5736.

Morin, P. and Samson, C. (2008a). Motion control of wheeled mobile robots. In *Springer Handbook of Robotics*, 799–826. Springer, Berlin.

Morin, P. and Samson, C. (2008b). Transverse function control of a class of non-invariant driftless systems. Application to vehicles with trailers. In *47th IEEE CDC*, 4312–4319. Cancun, Mexico.

Morro, A., Sgorbissa, A., and Zaccaria, R. (2011). Path following for unicycle robots with arbitrary path curvature. *IEEE Trans. on Robotics*, 27(5), 1016–1023.

Odhams, A., Roebuck, R., Lee, Y., and Cebon, D. (2009). Factors influencing the energy consumption of road freight transport. *Proc. IMechE. Part C: J. Mech. Eng. Science*, 224, 1995–2010.

Orosco-Guerrero, R., Aranda-Bricaire, E., and Velasco-Villa, M. (2002). Modeling and dynamic feedback linearization of a multi-steered N-trailer. In *IFAC 15th Triennial World Congress*.

Pradalier, C. and Usher, K. (2008). Robust trajectory tracking for a reversing tractor trailer. *J. Field Robot.*, 25(6-7), 378–399.

Rouchon, P., Fliess, M., Levine, J., and Martin, P. (1993). Flatness, motion planning and trailer systems. In *Proc. 32nd Conf. on Decision and Control*, 2700–2705. San Antonio, Texas.

Seron, M.M., Braslavsky, J.H., and Goodwin, G.C. (1997). *Fundamental limitations in filtering and control*. Springer, London.

Society of Automotive Engineers (2016). *Taxonomy and definitions for Terms Related to Driving Automation Systems for On-Road Motor Vehicles. Surface Vehicle Recommended Practice J3016*. SAE International.

Sørdalen, O. (1993). Conversion of the kinematics of a car with n trailers into a chained form. In *Proc. IEEE Int. Conf. on Robotics and Automation*, 382–387. Atlanta, USA.

Tilbury, D., rdalen, O.J.S., Bushnell, L., and Sastry, S.S. (1995). A multisteering trailer system: conversion into chained form using dynamic feedback. *IEEE Trans. Robot. Autom.*, 11(6), 807–818.

Vendittelli, M. and Oriolo, G. (2000). Stabilization of the general two-trailer system. In *Proceedings of the 2000 IEEE International Conference on Robotics and Automation*. San Francisco, CA.

Yoo, K. and Chung, W. (2010). Pushing motion control of n passive off-hooked trailers by a car-like mobile robot. In *2010 IEEE int. Conf. Robotics and Automation*, 4928–4933. Anchorage, USA.

Zabczyk, J. (1989). Some comments on stabilizability. In *Applied Mathematics and Optimization*, 1–9. Springer-Verlag, New York.